REPUBLIQUE ALGERIENNE DEMOCRATIQUE ET POPULAIRE

MINISTERE DE L'ENSEIGNEMENT SUPERIEUR ET DE LA RECHERCHE SCIENTIFIQUE

Université de Mohamed El-Bachir El-Ibrahimi - Bordj Bou Arreridj

Faculté *des Sciences et de la technologie*

Département d'Electronique

Mémoire

Présenté pour obtenir

LE DIPLOME DE MASTER

FILIERE : **Electronique**

Spécialité : Industries Electroniques

Par

- **SMAIL Islam**
- **BENKHALED Mohamed**

Intitulé

Approche robuste-intelligente pour le contrôle des convertisseurs DC-DC

Soutenu le : /06/2025

Devant le Jury composé de :

Nom & Prénom	*Grade*	*Qualité*	*Etablissement*
M.BELGIDOUM Khaoula	*MAA*	*Président*	*Univ-BBA*
M.TALBI Billel	*MCA*	*Encadreur*	*Univ-BBA*
M.ZERROUGUI Raouf	*MCB*	*Examinateur*	*Univ-BBA*

Année Universitaire 2024/2025

PEOPLE'S DEMOCRATIC REPUBLIC OF ALGERIA

MINISTRY OF HIGHER EDUCATION AND SCIENTIFIC RESEARCH

University Mohamed El-Bachir El-Ibrahimi - Bordj Bou Arreridj

Faculty of Science and Technology

Department of Electronics

Dissertation

Submitted in Partial Fulfillment of the Requirement

for an ACADEMIC MASTER DEGREE

FIELD: Electronic

Specialty: Electronic Industries

Submitted by:

- **SMAIL Islam**
- **BENKHALED Mohamed**

Titled

Robust-intelligent Approach for the Control of DC-DC Converters

Evaluated on: /06/2025

By the evaluation committee composed of :

Last & First name	*Grade*	*Quality*	*Establishment*
M.BELGIDOUM Khaoula	*MAA*	*President*	*Univ-BBA*
M.TALBI Billel	*MCA*	*Supervisor*	*Univ-BBA*
M.ZERROUGUI Raouf	*MCB*	*Examiner*	*Univ-BBA*

Academic Year 2024/2025

To the soul of my beloved grandfather – This work is a humble offering to your legacy, your kindness, and the quiet strength you passed on to me.

To my dear mother

To my dear father

To my family and those who stood by me

To my friends C.Mehdi , C.Fouad , N.Mourad , M.Abderrahmane.

To all who believed in me

Smail Islam

To my dear parents – your endless support, love, and prayers have been the foundation of every step I've taken. This work is a reflection of the values you've instilled in me.

To my family and loved ones – thank you for believing in me, especially during the most challenging moments.

To my friends – your companionship and encouragement made the path lighter and the days brighter.

To everyone who has supported, guided, or inspired me

this work is for you.

Benkaled Mohamed

Acknowledgment

*First and foremost, I thank **Allah** Almighty, the Most Gracious and the Most Merciful, for granting me the strength, patience, and determination to complete this work. Without His guidance and blessings, none of this would have been possible.*

*I would like to express my sincere gratitude to my supervisor, **Dr. Talbi billel**, for their valuable guidance, unwavering support, and continuous encouragement throughout the course of this research. Their insight and experience have been instrumental in shaping the direction and quality of this thesis.*

*My heartfelt thanks also go to **all the teachers and faculty members** who have contributed to my academic journey and helped me reach this stage. Your dedication to teaching and mentorship has laid the foundation for my success.*

*Special thanks are due to the **LEPCI** Laboratory group, whose resources, equipment, and technical support played a vital role in the practical implementation and experimental validation of this work. Your contributions are deeply appreciated.*

I am also thankful to my family, whose love, prayers, and unwavering belief in me have been my greatest source of strength and to my friends, who have stood by me through challenges and triumphs. To everyone who supported and believed in me

Finally, I extend my gratitude to everyone—seen and unseen—who has contributed to this work in ways big or small. This achievement is as much yours as it is mine.

Thank you from the bottom of my heart.

Abstract:

This thesis presents the modeling, simulation, and real-time implementation of advanced control strategies for a static DC-DC buck converter. Three controllers are designed and investigated: the conventional proportional-integral-derivative (PID) controller, the type-1 fuzzy logic controller (T1-FLC), and the type-2 fuzzy logic controller (T2-FLC). The work begins with a foundational review of Buck converter dynamics, followed by the development and simulation of the designed controllers using MATLAB®/Simulink®. Experimental validation is performed on the dSPACE DS1104 platform using ControlDesk software, under a range of test conditions including reference tracking, input voltage disturbances, and load variations. Comparative analysis reveals that the T2-FLC exhibits superior robustness, adaptability, and transient performance compared to both the classical PID and T1-FLC approaches.

Keywords: DC-DC Buck converter, PID controller, Type-1 and type-2 fuzzy logic controllers, Intelligent-robust control, Real-time implementation, dSPACE DS1104.

ملخص:

يعرض هذا العمل نمذجة، ومحاكاة، وتنفيذاً في الزمن الحقيقي لاستراتيجيات تحكم متقدمة في محول خافض للتيار المستمر(DC-DC Buck Converter). تم تصميم ودراسة ثلاثة متحكمات: المتحكم التقليدي التناسبي-التكاملي-التفاضليPID ، والمتحكم الضبابي من النوع الأولT1-FLC ، والمتحكم الضبابي من النوع الثاني T2-FLC. يبدأ العمل بمراجعة أساسية لديناميكيات محولBuck ، تليها عملية تطوير ومحاكاة للمتحكمات المصممة باستخدام برنامج MATLAB®/Simulink®. تم تنفيذ التحقق التجريبي باستخدام منصة dSPACE DS1104 وبرنامجControlDesk ، تحت مجموعة متنوعة من ظروف الاختبار، بما في ذلك تتبع الإشارة المرجعية، اضطرابات جهد الدخل، وتغيرات الحمل. وقد أظهرت التحليلات المقارنة أن المتحكم الضبابي من النوع الثاني T2-FLC يوفر أداءً أعلى من حيث المتانة، والقدرة على التكيف، والاستجابة الانتقالية مقارنة بالمتحكم PID الكلاسيكي والمتحكم الضبابي من النوع الأولT1-FLC .

الكلمات المفتاحية:

محول خافضDC-DC ، متحكمPID ، المتحكمات الضبابية من النوع الأول والنوع الثاني، تحكم ذكي ومتين، تنفيذ في الزمن الحقيقي،dSPACE DS1104.

Résumé :

Ce mémoire présente la modélisation, la simulation et l'implémentation en temps réel de stratégies de commande avancées pour convertisseur statique DC-DC de type Buck. Trois régulateurs sont conçus et étudiés : le régulateur proportionnel-intégra-dérivé (PID) classique, le régulateur flou de type 1 (T1-FLC) et le régulateur flou de type 2 (T2-FLC). Le travail commence par une étude fondamentale de la dynamique du convertisseur Buck, suivie par le développement et la simulation des régulateurs conçus à l'aide de MATLAB®/Simulink®. La validation expérimentale est réalisée sur la plateforme dSPACE DS1104 à l'aide du logiciel ControlDesk, dans diverses conditions de test incluant le suivi de référence, les perturbations de la tension d'entrée et les variations de charge. L'analyse comparative montre que le régulateur flou de type 2 présente une robustesse, une adaptabilité et des performances transitoires supérieures par rapport aux approches PID classique et T1-FLC.

Mots-clés : Convertisseur DC-DC Buck, Régulateur PID, Régulateurs flous de type 1 et de type 2, Commande robuste-intelligente, Implémentation en temps réel, dSPACE DS1104.

Summary

Chapter III : Real-time Implementation of Synthesized Controllers

List of Figures

List of Tables

List of Acronyms

ANN	Artificial Neural Networks
DC	Direct current
CCM	Continuous conduction mode
DCM	DISCONTINUOUS CONDUCTION MODE
DSP	Digital signal processor
FLC	Fuzzy Logic Controller
FOU	Footprint of uncertainty
IAE	Integral of Absolute Error
IGBT	Insulated gate bipolar transistor
ISE	Integral of Squared Error
ITAE	Integral of Time-weighted Absolute Error
ITSE	Integral of Time-weighted Squared Error
LMF	Lower membership function
LQR	Linear Quadratic Regulator
PID	Proportional-Integral-Derivative
PWM	Pulse width modulation
T1-FLC	Type 1 Fuzzy Logic Controller
T2-FLC	Type 2 Fuzzy Logic Controller
UMF	Upper membership function

List of Symbols

δ, β	fraction of the switching period
i_L	inductor current
T	switching period
L	inductance
C	capacitance
R	Resistive Load
v_{out}	Output voltage
v_L	Inductor voltage
α	duty cycle
Δi_L	Inductor current ripple
ΔV_{out}	Inductor voltage ripple
$I_{L,avg}$	Average inductor current
I_{max}	Peak inductor current
I_{min}	Minimum inductor current
v_{in}	Input voltage
f_{sw}	switching frequency
$\tilde{\imath}_L, \tilde{v}_{in}, \tilde{v}_{out}, \tilde{\alpha}$	small perturbation
K_p	Proportional gain
K_i	Integral gain
p_1, p_2, p_3	desired pole
ζ	damping ratio
ω_n	natural frequency
$\tilde{A}$	fuzzy set
$\mu_{\tilde{A}}(x)$	membership function of type 1
k_e, k_{de}, k_p, k_i	coefficients of normalization
$\mu_{\tilde{A}}(x, u)$	membership function of type 2

General Introduction

In modern power electronic systems, precise, efficient, and adaptable control has become not just a design requirement but a foundational necessity. The widespread integration of DC-DC converters, particularly in embedded and mobile applications such as electric vehicles, renewable energy systems, aerospace power supplies, and telecommunications, has redefined how we manage electrical energy at the system level [1]. This shift is largely due to the advantages of DC-DC converters, including minimal power losses and excellent dynamic response, which enable the development of faster, more compact, and more reliable energy conversion platforms [2].

Among various DC-DC converter topologies, the Buck converter remains one of the most widely used topologies due to its simplicity, efficiency, and ability to step down voltage in a controlled manner. However, ensuring precise output regulation under variable conditions, such as load disturbances, input voltage fluctuations, or component tolerances, requires advanced control strategies. Traditional control methods, like PID controllers, although simple and effective in many scenarios, often struggle in highly nonlinear or uncertain environments. This limitation has sparked interest in intelligent control techniques that emulate human reasoning and handle uncertainty and imprecision more effectively [3].

In this context, fuzzy logic controller (FLC) presents a compelling alternative. By operating on linguistic variables and rules derived from expert knowledge, FLCs offer nonlinear, model-free control that can adapt to real-world complexity. The evolution from type-1 to type-2 fuzzy systems marks a significant paradigm shift. Type-2 FLCs extend the capabilities of their type-1 counterparts by modeling uncertainty within the membership functions themselves, thereby capturing imprecise, vague, or conflicting information with greater fidelity. This is particularly valuable when sensor noise, unmodeled dynamics, or ambiguity in expert knowledge challenge the limits of classical control logic [4].

In this thesis, three control strategies, PID, type-1 FLC, and type-2 FLC, are investigated to regulate the output of a DC-DC Buck converter. Their performance is evaluated through both simulation and real-time experimental implementation using the dSPACE DS1104 platform. The objective of this study is to demonstrate the practical viability of intelligent fuzzy

controllers, with a particular emphasis on type-2 system, as a robust and effective solution to the complex control challenges inherent in modern power electronic applications.

The details description of this thesis is compiled into 3 chapters:

- Chapter I: introduces the theoretical and operational principles of DC-DC converters, with a particular focus on the Buck converter topology. Additionally, the design and simulation of a PID controller for the Buck converter are discussed in detail.
- Chapter II: presents a detailed study of fuzzy logic controllers applied to the Buck converter explaining their architecture, rule base design, and defuzzification mechanisms. A comprehensive comparative simulation study is conducted between the designed PID controller, type-1 FLC, and type-2 FLC. The controllers are evaluated under various scenarios, including nominal operating conditions, load resistance variations, output voltage tracking with different reference profiles, and input voltage disturbances.
- Chapter III: focuses on the real-time implementation of the designed controllers using the dSPACE DS1104 platform and ControlDesk software. The same test scenarios used in the simulation study are considered to validate and verify the effectiveness and robustness of the designed controllers.

Finally, a general conclusion of this work and perspectives are listed at the end.

Chapter I:

Generalities on DC-DC Converters

I.1 Introduction

This chapter provides a foundational analysis of DC-DC static converters, with a particular emphasis on the Buck converter; a topology employed for step-down voltage regulation in power electronic systems. As demands for energy efficiency, compact design, and precise voltage control become increasingly critical across applications ranging from embedded systems to renewable energy, a deep understanding of converter operation is essential for robust controller design [5].

We begin by detailing the fundamental operating principles of DC-DC converters and identifying the key electrical parameters that influence their dynamic behavior. In addition, this chapter provides a brief review of control strategies applicable to DC-DC converters. The Buck converter is employed as a practical case study due to its prevalence in regulated DC power supplies. Building on this, the chapter explores a conventional control strategy, the PID controller, recognized for its straightforward implementation and broad industrial adoption.

I.2. DC-DC Converters

A chopper or DC-DC converter is a power electronics device that employs one or more controlled switches to change the voltage level. When the output voltage is lower than the input voltage, the converter is called a Buck converter. Conversely, if the output voltage is higher than the input voltage, it is called a Boost converter. Some choppers are capable of working in both modes, these are known as Buck-Boost converters. Certain choppers are also reversible, meaning they can supply energy to the load or absorb energy from it, enabling regenerative braking [2].

I.2.1. Operating Principle

As seen in Figure I.1, the fundamental idea of a DC-DC converter is to take an input voltage v_{in} and convert it into an output voltage v_{out}, which may be higher, lower, or inverted relative to the input. This is achieved through different circuit topologies, such as the Buck converter (Step-down), the Boost converter (Step-up), and the Buck-Boost converter (Step-up/down or inverted). DC-DC converters can operate in two conduction modes depending on its energy storage capacity, switching period and load, namely continuous conduction mode (CCM) and discontinuous conduction mode (DCM) [6].

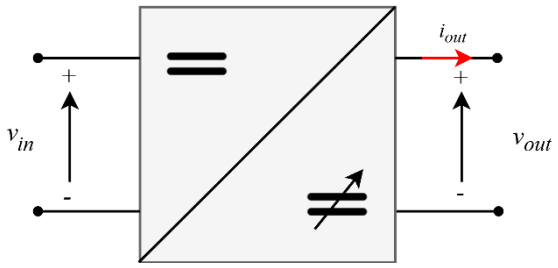

Figure I.1. DC- DC converter.

I.2.1.1. Continuous Conduction Mode

In this mode, the energy stored in the inductance L is partially transferred during each switching period. The converter can remain in this mode as long as the storage time of the inductor is relatively long. Figure I.2(a) illustrates the inductor current i_L for a converter operating in CCM. In this case, the conduction time of the active switch is noted as αT, where α represents the duty cycle and T is the switching period. A key feature of CCM is that its inductive current i_L is always positive [7].

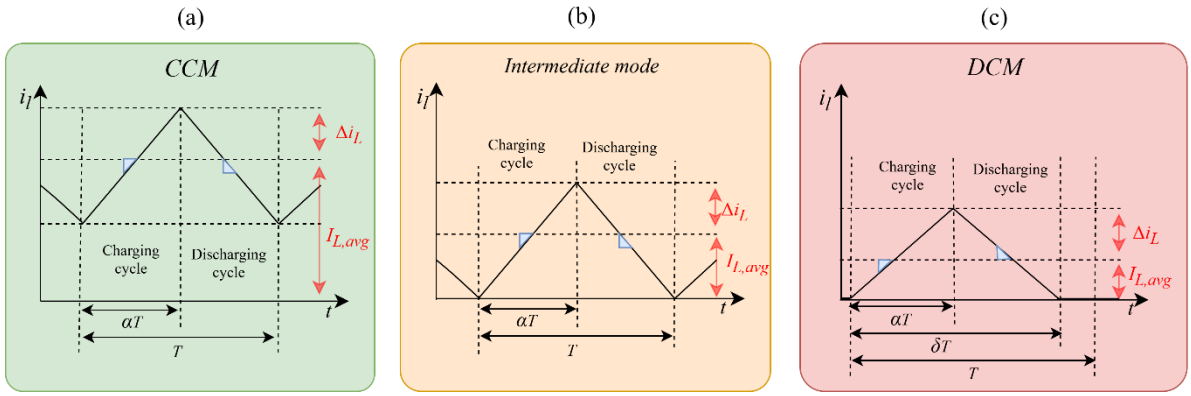

Figure I.2. Transition from continuous conduction to discontinuous conduction: (a) CCM mode, (b) Intermediate mode and CCM mode.

I.2.1.2. Discontinuous Conduction Mode

If the inductance is relatively small, or if the switching period is relatively long, the inductor current i_L may drop to zero before the end of the switching period T, as shown in Figure I.2(c).

This is a "dead" phase during which no energy transfer takes place from the source to the charge and the capacitor then slowly discharges through the load resistance. In such cases, the converter is said to operate in DCM. The duration of the conduction interval, when $i_L \neq 0$, is denoted by δT, where δ represents the fraction of the switching period during which the inductor current i_L is nonzero. Consequently, the duration of the no-conduction interval is given by $\beta T = T - \delta T$, where β is the fraction of the switching period during which $i_L \neq 0$.

I.2.2. Classification of DC-DC Converters

Main types of DC-DC converters include the Buck converter, Boost converter, and Buck-Boost converter, each with its own advantages and specific applications in the technological field [6].

I.2.2.1. Buck Converter

A Buck converter, or series chopper, is a switching power supply that converts one DC voltage into another lower-value DC voltage. It is used for applications where the voltage is adjustable but always lower than that present at the input. Figure I.3 shows the electrical diagram of the Buck converter.

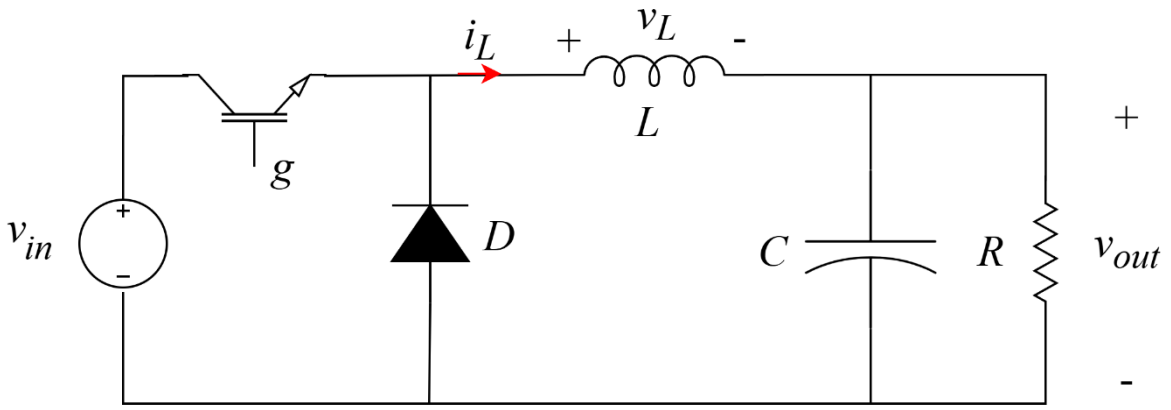

Figure I.3. Electrical circuit of the Buck converter.

The inductance L and the capacitance C form a second order filter, which ensures excellent filtering of the voltage v_{out} applied to the load R. The operation of the converter is governed by the switching state of the active power switch and can be divided into two main modes:

- *First Case* (*Switch ON* $g = 1$): When the active switch is closed (ON), the input voltage v_{in} is directly applied across the inductor. As a result, the current through the inductor i_L increases. Since the voltage at the diode is negative during this state, the diode is reverse-biased and therefore does not conduct. The voltage across the inductor v_L is given by:

$$v_L = v_{in} - v_{out} \tag{I.1}$$

- *Second Case* (*Switch OFF* $g = 0$): When the switch is open (OFF), the inductor maintains the current flow by forward-biasing the diode, which allows current to continue flowing to the load. In this state, the current through the inductor i_L decreases, and the inductor releases stored energy. The voltage across the inductor v_L is then:

$$v_L = -v_{out} \tag{I.2}$$

Tables I.1 and I.2 summarize the key equations of the Buck converter in both CCM and DCM modes, respectively.

Table I.1. Key equations of the Buck converter in CCM mode.

Parameter	Equation	Notes
Output Voltage v_{out}	$v_{out} = \alpha v_{in}$	Linear relation with duty cycle α
Inductor Current Ripple Δi_L	$\Delta i_L = v_{in}\left(\frac{1-\alpha}{L}\right)\alpha T$	Depends on L, T, and α
Average Inductor Current $I_{L,avg}$	$I_{L,avg} = \frac{I_{max}+I_{min}}{2} = \frac{v_{out}}{R}$	Matches load current
Peak Inductor Current I_{max}	$I_{max} = \frac{v_{out}}{R} + \frac{\Delta i_L}{2}$	Occurs at the end of the switch-on interval αT
Minimum Inductor Current I_{min}	$I_{min} = \frac{v_{out}}{R} - \frac{\Delta i_L}{2}$	Must be > 0 for CCM
Condition For CCM	$I_{min} > 0$	Ensures i_L never drops to zero

Table I.2. Key equations of the Buck converter in DCM mode.

Parameter	Equation	Notes
Output Voltage v_{out}	$v_{out} = \frac{\alpha^2}{\alpha^2 + \frac{1}{4}\left(\frac{I_{out,avg}}{I_{L_{min},max}}\right)} v_{in}$	Non-linear, load-dependent. With $I_{out,avg} = I_{L,avg}$ and $I_{L_{min},max} = \frac{V_{in}T}{8L}$
Inductor Current Ripple Δi_L	$\Delta i_L = \frac{v_{out}}{L}\Delta T$	ΔT is the conduction interval of the diode ($\Delta T = \delta T - \alpha T$)
Average Inductor Current $I_{L,avg}$	$I_{L,avg} = \frac{I_{max}(\alpha + \Delta)}{2}$	Depends on peak current and conduction intervals
Peak Inductor Current I_{max}	$I_{max} = \left(\frac{v_{in} - v_{out}}{L}\right)\alpha T$	Occurs at the end of the switch-on interval αT
Condition For DCM	$I_{min} = 0$	i_L reaches zero before T ends

I.2.2.2. Boost Converter

A Boost converter, or parallel chopper, is a switching power supply that converts one DC voltage into another higher-regulated DC voltage. A boost converter increases the voltage supplied by the batteries and thus reduces the number of elements required to reach the desired voltage level. Hybrid vehicles and lighting systems are two typical examples of the use of Boost converter. Figure I.4 shows the electrical diagram of the converter [6].

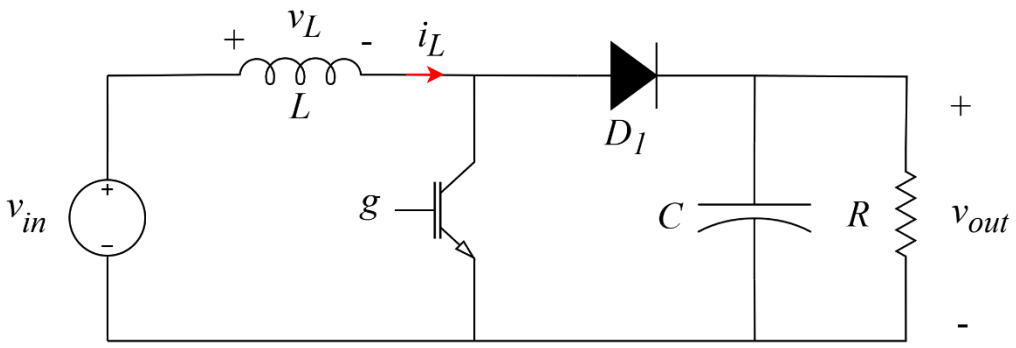

Figure I.4. Electrical circuit of the Boost converter.

A Boost converter operates in two phases to step up the input voltage. In the first phase, when the switch is closed (ON), current flows through the inductor, and energy is stored as a magnetic field while the load is temporarily isolated due to the reverse-biased diode. In the second phase, when the switch is opened (OFF), the inductor releases its stored energy, which adds to the input voltage and forward-biases the diode, allowing current to flow through the output capacitor and supply the load. This process results in an output voltage higher than the input voltage. The key equations of the Boost converter in both CCM and DCM modes are presented in Tables I.3 and I.4, respectively.

Table I.3. Key equations of the Boost converter in CCM mode.

Parameter	Equation	Notes
Output Voltage v_{out}	$v_{out} = \frac{1}{1-\alpha} v_{in}$	Output increases with duty cycle α; non-linear gain.
Inductor Current Ripple Δi_L	$\Delta i_L = \frac{v_{in}}{L} \alpha T$	Depends on L, T, and α
Average Inductor Current $I_{L,avg}$	$I_{L,avg} = \frac{v_{in}}{R} \frac{1}{(1-\alpha)^2}$	Reflects increased current demand from input
Peak Inductor Current I_{max}	$I_{max} = \frac{v_{out}}{R} + \frac{\Delta i_L}{2}$	Occurs at the end of the switch-on interval αT
Minimum Inductor Current I_{min}	$I_{min} = \frac{v_{out}}{R} - \frac{\Delta i_L}{2}$	Must be > 0 for CCM
Condition For CCM	$I_{min} > 0$	Ensures i_L never drops to zero

Table I.4. Key equations of the Boost converter in DCM mode.

Parameter	Equation	Notes
Output Voltage v_{out}	$v_{out} = \frac{v_{in}}{2} + \frac{v_{in}}{2}\sqrt{1 + \frac{2\alpha^2 TR}{L}}$	Dependent on load and inductor size; lower than CCM case.
Inductor Current Ripple Δi_L	$\Delta i_L = \frac{v_{out} - v_{in}}{L}\Delta T$	ΔT is the conduction interval of the diode ($\Delta T = \delta T - \alpha T$)
Average Inductor Current $I_{L,avg}$	$I_{L,avg} = \frac{I_{max}(\alpha + \Delta)}{2}$	Depends on peak current and conduction intervals
Peak Inductor Current I_{max}	$I_{max} = \frac{v_{in}}{L}\alpha T$	Occurs at the end of the switch-on interval αT
Condition For DCM	$I_{min} = 0$	i_L reaches zero before T ends

I.2.2.3. Buck-Boost Converter

A Buck-Boost converter is a versatile DC-DC converter that can both step up and step-down voltage by adjusting the duty cycle. It operates in inverting or non-inverting modes, depending on the application's polarity needs. Key design parameters such as duty cycle, switching frequency, and inductance affect output regulation and efficiency, making it ideal for systems with fluctuating input voltages, like battery-powered or renewable energy devices [6].

a. Inverting Buck-Boost Converter

Figure I.5 shows the electrical diagram of this type of converter. The input voltage could be either higher or lower than the desired output voltage. Indeed, if the duty cycle α is greater than 50% the chopper works in boost mode and if α is less than 50% the chopper works in buck mode. The inverting Buck-Boost converter has a negative output relative to the input voltage. Tables I.5 and I.6 give the key equations of the inverting Buck-Boost converter in both CCM and DCM modes, respectively [6].

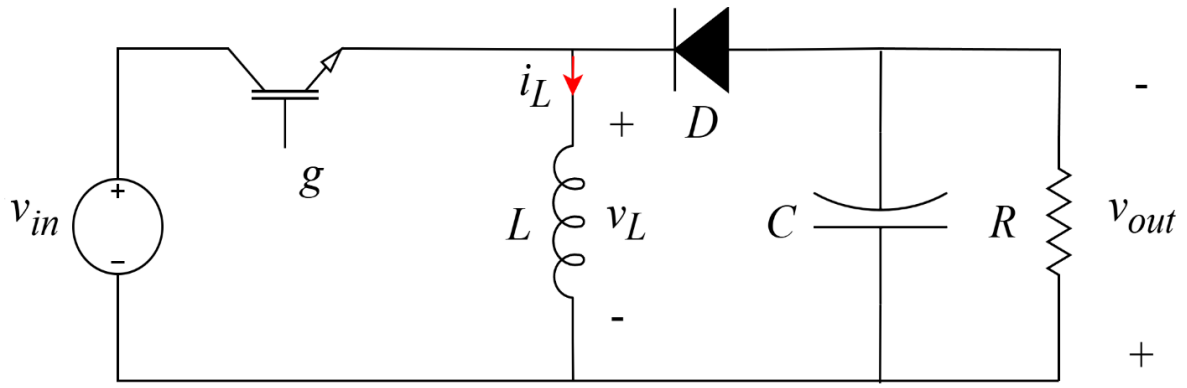

Figure I.5. Electrical circuit of the inverting Buck-Boost converter.

Table I.5. Key equations of the inverting Buck-Boost converter in CCM mode.

Parameter	Equation	Notes
Output Voltage v_{out}	$v_{out} = -\frac{\alpha}{1-\alpha} v_{in}$	Negative output voltage; step-up/step-down depending on α
Inductor Current Ripple Δi_L	$\Delta i_L = \frac{v_{in}}{L} \alpha T$	Depends on L, T, and α
Average Inductor Current $I_{L,avg}$	$I_{L,avg} = \frac{v_{out}}{R(1-\alpha)}$	Scales with output current and α
Peak Inductor Current I_{max}	$I_{max} = \frac{v_{out}}{R(1-\alpha)} + \frac{\Delta i_L}{2}$	Occurs at the end of the switch-on interval αT
Minimum Inductor Current I_{min}	$I_{min} = \frac{v_{out}}{R(1-\alpha)} - \frac{\Delta i_L}{2}$	Must be > 0 for CCM
Condition For CCM	$I_{min} > 0$	Ensures i_L never drops to zero

Table I.6. Key equations of the inverting Buck-Boost converter in DCM mode.

Parameter	Equation	Notes
Output Voltage v_{out}	$v_{out} = -v_{in}\alpha\sqrt{\frac{RT}{2L}}$	Negative output voltage depends on duty cycle α, R load and period T
Inductor Current Ripple Δi_L	$\Delta i_L = \frac{v_{in}}{L} \Delta T$	ΔT is the conduction interval of the diode ($\Delta T = \delta T - \alpha T$)
Average Inductor Current $I_{L,avg}$	$I_{L,avg} = \frac{I_{max}(\alpha + \Delta)}{2}$	Derived assuming a linear ramp from 0 to I_{max}
Peak Inductor Current I_{max}	$I_{max} = \frac{v_{in}}{L} \alpha T$	Occurs at the end of the switch-on interval αT
Condition For DCM	$I_{min} = 0$	i_L reaches zero before T ends

b. Non-inverting Buck-Boost Converter

The non-inverting Buck-Boost converter is a serial combination of a Buck and Boost converter. It can be used in either boost mode or buck mode or buck-boost mode by controlling the duty cycle α of the circuit. Figure I.6 shows the circuit of this converter [6].

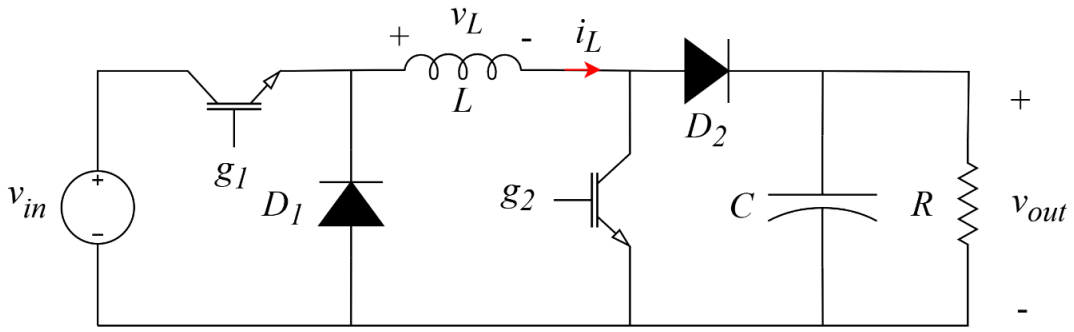

Figure I.6. Electrical circuit of the non-inverting Buck-Boost converter.

The key equations of the non-inverting Buck-Boost converter in both CCM and DCM modes are presented in Tables I.7 and I.8, respectively.

Table I.7. Key equations of the non-inverting Buck-Boost converter in CCM mode.

Parameter	Equation	Notes
Output Voltage v_{out}	$v_{out} = \frac{\alpha}{1-\alpha} v_{in}$	Positive output voltage; step-up/step-down depending on α
Inductor Current Ripple Δi_L	$\Delta i_L = \frac{v_{in}}{L} \alpha T$	Depends on L, T, and α
Average Inductor Current $I_{L,avg}$	$I_{L,avg} = \frac{v_{out}}{R(1-\alpha)}$	Scales with output current and α
Peak Inductor Current I_{max}	$I_{max} = \frac{v_{out}}{R(1-\alpha)} + \frac{\Delta i_L}{2}$	Occurs at the end of the switch-on interval αT
Minimum Inductor Current I_{min}	$I_{min} = \frac{v_{out}}{R(1-\alpha)} - \frac{\Delta i_L}{2}$	Must be > 0 for CCM
Condition For CCM	$I_{min} > 0$	Ensures i_L never drops to zero

Table I.8. Key equations of the non-inverting Buck-Boost converter in DCM mode.

Parameter	Equation	Notes
Output Voltage v_{out}	$v_{out} = v_{in} \alpha \sqrt{\frac{RT}{2L}}$	Positive output voltage depends on duty cycle α, R load, and period T
Inductor Current Ripple Δi_L	$\Delta i_L = \frac{v_{in}}{L} \Delta T$	ΔT is the conduction interval of the diode ($\Delta T = \delta T - \alpha T$)
Average Inductor Current $I_{L,avg}$	$I_{L,avg} = \frac{I_{max}(\alpha + \Delta)}{2}$	Derived assuming a linear ramp from 0 to I_{max}
Peak Inductor Current I_{max}	$I_{max} = \frac{v_{in}}{L} \alpha T$	Occurs at the end of the switch-on interval αT
Condition For DCM	$I_{min} = 0$	i_L reaches zero before T ends

I.3. Control Techniques of DC-DC Converters

The control unit serves as the brain of the DC-DC converter, while the converter is treated as the heart. Its primary role is to ensure that the converter delivers a regulated output voltage suitable for the connected load. However, due to the disturbances occurring in the converter, such as input voltage fluctuations and load variations, the load is always not getting the desired output voltage. As a result, closed-loop control becomes indispensable to maintain voltage regulation and ensure stable operation under all conditions [8].

There are various kinds of control techniques used for the DC-DC converters to improve their dynamic performance and stability, under varying operating conditions. These techniques may be categorized into two classes: classical controllers and advanced controllers, as illustrated in Figure I.7 [7].

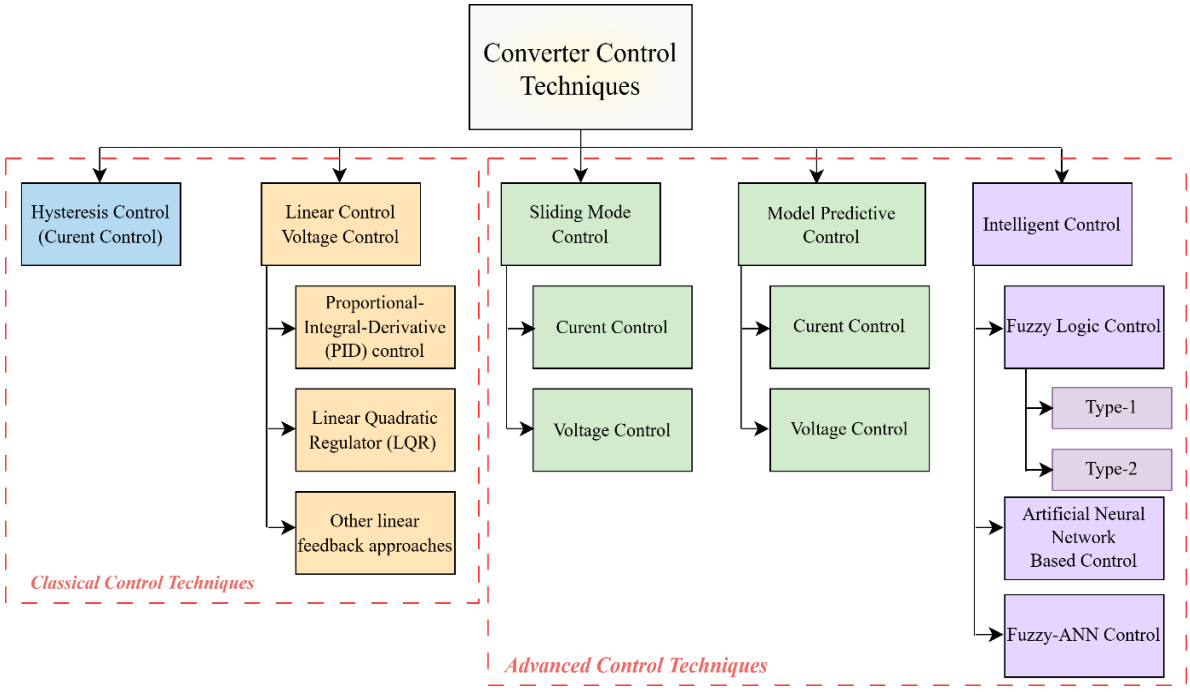

Figure I.7. Classification of control techniques used for the DC-DC converters.

Classical control techniques include well-established methods such as hysteresis control and linear control, which further branch into specific strategies like Proportional-Integral-Derivative (PID) control, Linear Quadratic Regulator (LQR), and other linear feedback approaches. These techniques are known for their simplicity, and ease of implementation. However, they often exhibit degraded performance in the presence of parameter variations and external disturbances, limiting their effectiveness in complex or highly dynamic systems. On the other hand, advanced control techniques encompass modern, intelligent, and model-based approaches. This category includes methods such as Sliding Mode Control and Model Predictive Control. In addition, Intelligent Control incorporates strategies like Fuzzy Logic Type-1 and Type-2, Artificial Neural Networks (ANNs), and hybrid Fuzzy-ANN control, offering enhanced adaptability and robustness in handling nonlinearities, uncertainties, and varying operating conditions.

Fuzzy control offers several practical advantages over other intelligent control techniques, particularly in power electronics applications. Unlike neural networks, fuzzy logic does not require extensive training data. Instead, it relies on intuitive rule-based reasoning, making it

easier to design, interpret, and tune. Fuzzy controllers are inherently robust to system uncertainties and nonlinearities, and they perform well even with imprecise or incomplete models ideal for real-world systems where exact dynamics are difficult to capture. Moreover, implementation is relatively lightweight in terms of computational resources, which makes fuzzy control well-suited for embedded and real-time systems, especially where fast, adaptive regulation is essential.

I.4. Modeling a Buck Converter

The Buck converter combines linear and nonlinear components, making its dynamic behavior nonlinear and time-varying due to switching actions. To simplify control design, a small-signal model is derived using the state-space averaging method, which averages system dynamics over a switching cycle and linearizes it around a steady-state point.

I.4.1. Buck Converter Model

Figure I.8 illustrates the equivalent circuits of the Buck converter corresponding to the ON and OFF states of the active switch, with the inductor current i_L and the output voltage and v_{out} selected as the state variables. The converter is assumed to operate in CCM mode.

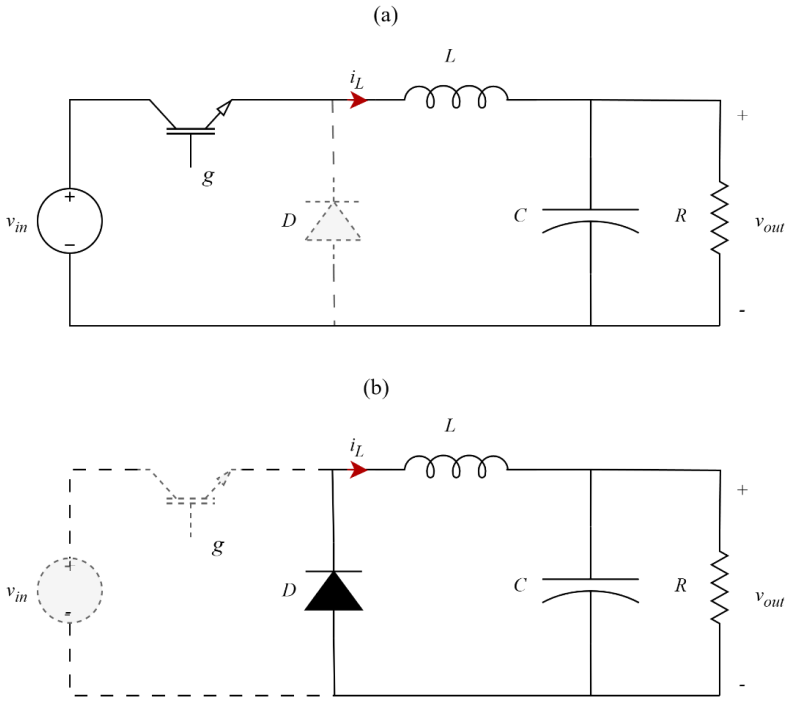

Figure I.8. Equivalent Buck circuit: (a) ON state; (b) OFF state.

- ON state $t \in [0 \rightarrow \alpha T]$: During the ON interval, the active switch is conducting, and the diode is reverse-biased (open circuit), as shown in Figure I.8(a). The state-space equations governing the system are:

$$\begin{cases} L\dfrac{di_L}{dt} = v_{in} - v_{out} \\ C\dfrac{dv_{out}}{dt} = i_L - \dfrac{v_{out}}{R} \end{cases} \quad \text{(I.3)}$$

- OFF state $t \in [\alpha T \rightarrow T]$: During the OFF interval, the active switch is open and the diode conducts, as shown in Figure I.8(b). The state-space equations become:

$$\begin{cases} L\dfrac{di_L}{dt} = -v_{out} \\ C\dfrac{dv_{out}}{dt} = i_L - \dfrac{v_{out}}{R} \end{cases} \quad \text{(I.4)}$$

The averaged state-space equations over one switching period can be obtained by multiplying equation (I.3), corresponding to the ON state, by the duty cycle α, and equation (I.4), corresponding to the OFF state, by $(1-\alpha)$. By summing the two weighted equations, the averaged model of the Buck converter is given as follows:

$$\begin{cases} L\dfrac{di_L}{dt} = \alpha v_{in} - v_{out} \\ C\dfrac{dv_{out}}{dt} = i_L - \dfrac{v_{out}}{R} \end{cases} \quad \text{(I.5)}$$

I.4.2. Design of the Buck Converter

The Buck converter is designed to supply a resistive load of 15Ω. The input voltage V_{in} is set to 48 V, and the desired output voltage v_{out} is 12V. Based on the basic voltage conversion ratio of a Buck converter, the required duty cycle α is calculated as:

$$\alpha = \frac{v_{out}}{V_{in}} = 0.25 \quad \text{(I.6)}$$

The inductor value is selected to ensure that the peak-to-peak inductor current ripple Δi_L remains within 10% of the input current, at a switching frequency $f_{sw} = \frac{1}{T} = 10kHz$. The average inductor current $I_{L,avg}$ is calculated as:

$$I_{L,avg} = \frac{v_{out}}{R} = 0.8\ A \quad \text{(I.7)}$$

Thus, the ripple current Δi_L is:

$$\Delta i_L = 0.08A \quad \text{(I.8)}$$

Using this value, the required inductance is determined by:

$$L = V_{in}\left(\frac{1-\alpha}{\Delta i_L}\right)\alpha T = 11.25\ mH \quad \text{(I.9)}$$

Similarly, the output capacitor is chosen to limit the output voltage ripple Δv_{out} to within 0.1% of the nominal output voltage:

$$C = \frac{(1-\alpha)}{8L(\Delta v_{out}/v_{out})f_{sw}^2} = 83.33\ \mu F \tag{I.10}$$

To ensure availability of components, normalized values of $L = 10\ mH$ and $C = 110\ \mu F$ are selected for the simulation tests.

I.4.3. Design of the PID Controller

Figure I.9 shows the control scheme of the Buck converter with a PID controller. The input to the PID controller is the error signal, defined as the difference between the output voltage and its reference value. The output of the PID controller is the duty cycle α, which serves as the input to the PWM modulator responsible for generating the switching signal g. A properly designed control loop ensures system stability and provides a fast dynamic response. The design of the voltage control loop involves the design of PID controller parameters.

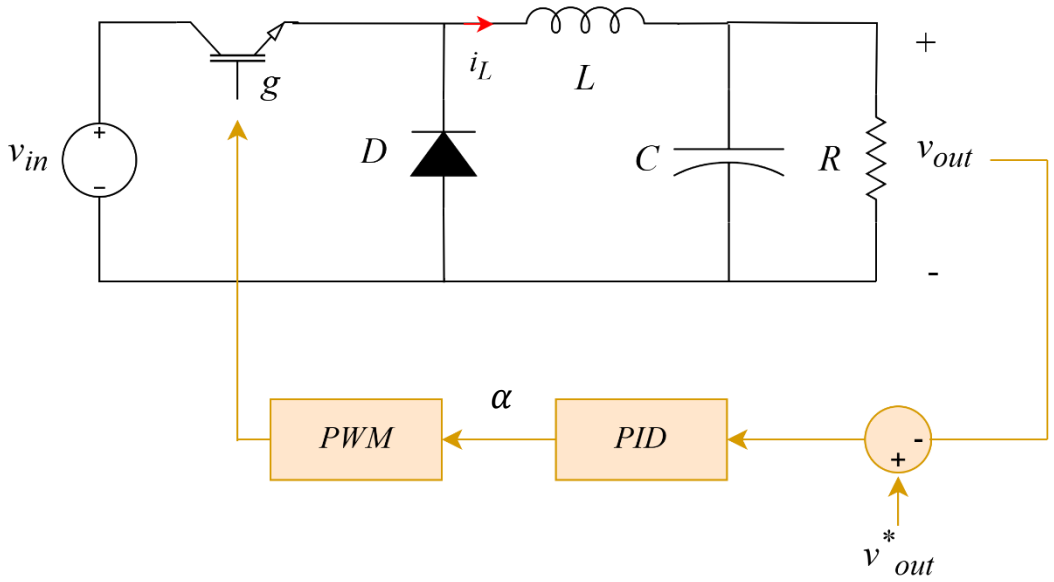

Figure I.9. Control scheme for the Buck converter using PID controller.

Introducing small perturbation around the steady-state value for the state variables and other quantities such that $i_L = I_L + \tilde{\imath}_L$, $v_{in} = V_{in} + \tilde{v}_{in}$, $v_{out} = V_{out} + \tilde{v}_{out}$, and $\alpha = A + \tilde{\alpha}$, the linearized small-signal model of the Buck converter is described by the following equations:

$$\begin{cases} L\dfrac{d\tilde{\imath}_L}{dt} = \tilde{\alpha}V_{in} + A\tilde{v}_{in} - \tilde{v}_{out} \\ C\dfrac{d\tilde{v}_{out}}{dt} = \tilde{\imath}_L - \dfrac{\tilde{v}_{out}}{R} \end{cases} \tag{I.11}$$

where $\tilde{\imath}_L$, $\tilde{v}_{in}$, $\tilde{v}_{out}$, and $\tilde{\alpha}$ are small perturbations in inductor current, input voltage, output voltage, and duty cycle α, respectively.

Applying the Laplace transform, the control-to-output transfer function of the Buck converter is obtained as:

$$G_{BC}(s) = \frac{\tilde{v}_{out}}{\tilde{\alpha}} = \frac{V_{in}}{LCs^2 + \frac{L}{R}s + 1} \tag{I.12}$$

The transfer function of the PID controller, neglecting the derivative term for simplification ($\alpha = 0$), is given by:

$$G_{co}(s) = K_p + \frac{K_i}{s} \tag{I.13}$$

The closed-loop transfer function of the PID-controlled Buck converter is given by

$$G_{CL}(s) = \frac{G_{co}(s)G_{BC}(s)}{1 + G_{co}(s)G_{BC}(s)} = \frac{V_{in}(K_i + K_p s)}{LCs^3 + \frac{L}{R}s^2 + (1 + K_p V_{in})s + V_{in}K_i} \tag{I.14}$$

The nominal parameters of the Buck converter are summarized in Table I.9, and the corresponding Bode plot of the control loop is shown in Figure I.10(a). The closed-loop transfer function corresponds to a third-order system, and a PID controller was implemented to enhance system stability**.** The controller gains ($K_p = 0.04$ and $K_i = 20.673$)were selected based on a desired dominant pole located at $p_1 = -376$ (corresponding to a damping ratio $\zeta = 1$ and natural frequency $\omega_n = 376\, rad/s$), along with a pair of complex conjugate poles at $p_{2,3} = -115 \pm j721$ (yielding $\zeta = 0.607$ and $\omega_n = 730\, rad/s$). This pole placement ensures a fast transient response with moderate damping.

Table I.9. Nominal parameters of the Buck converter.

Parameter	Symbol	Value
Input Voltage	v_{in}	48 V
Inductor	L	10mH
Capacitor	C	110µF
Load Resistance	R	15Ω
Switching Frequency	f_{sw}	10kHz

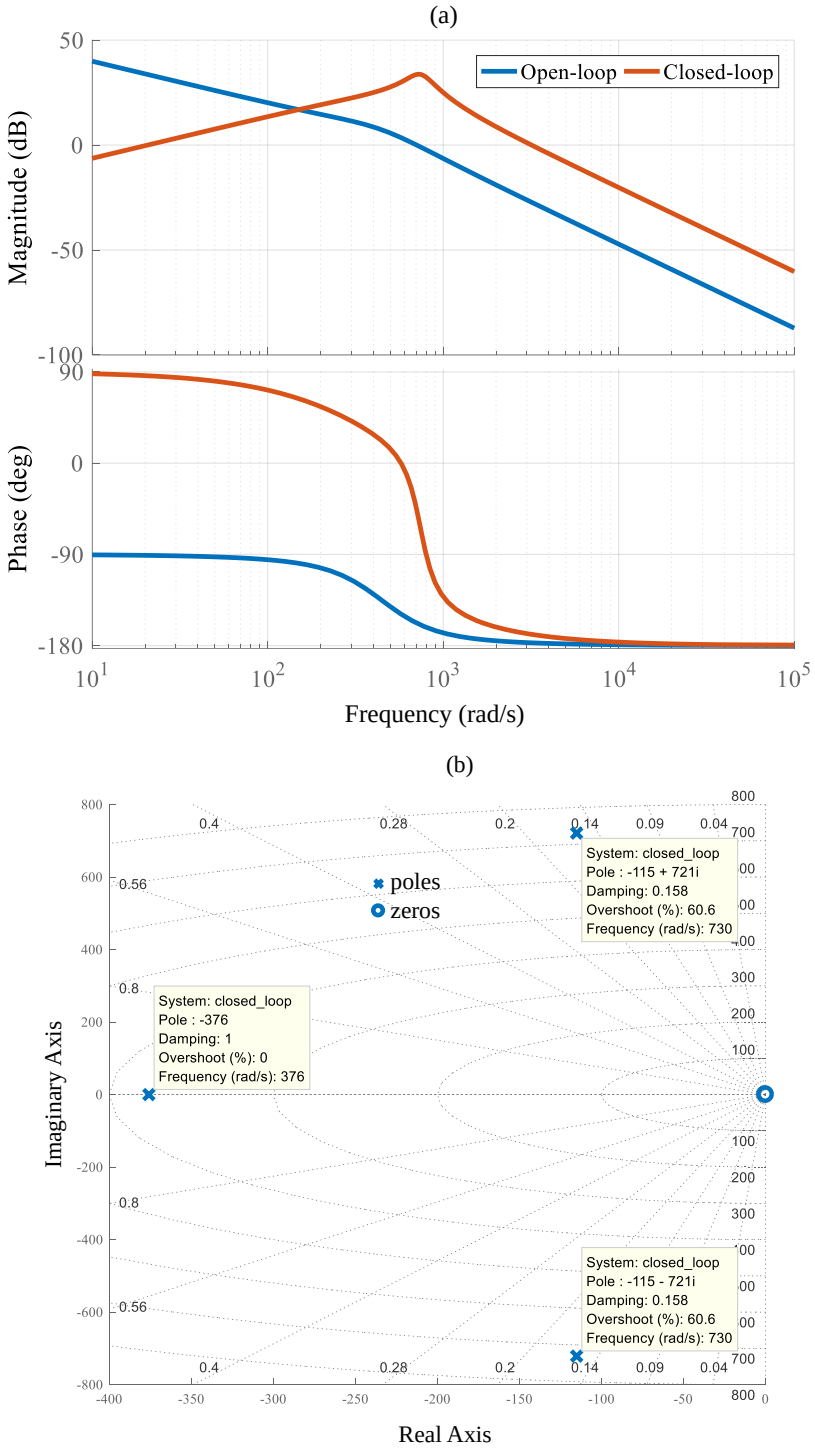

Figure I.10. (a) Bode plot of the transfer function of the PID-controlled Buck converter and (b) Poles and zeros of the closed-loop system

I.4.4. Simulation Results

MATLAB®/Simulink® is used to implement and simulate the designed PID Controller, in conjunction with the Simscape Power Systems package (formerly known as SimPowerSystems) to model the Buck converter. The parameters of the Buck converter are provided in Table I.9, and the PID controller gains are listed in the previous section.

Figure I.11 presents the simulation results for the output voltage and inductor current of the Buck converter, which is controlled using the designed PID controller. The system operates under a fixed reference output voltage of 12 V. It can be observed that the response stabilizes at 12 V with a settling time of 23.2 milliseconds, following a short period of oscillation. The key performance parameters corresponding to these results are listed in Table I.10, including the IAE (Integral of Absolute Error), ISE (Integral of Squared Error), $ITAE$ (Integral of Time-weighted Absolute Error) and $ITSE$ (Integral of Time-weighted Squared Error) error indices. The mathematical expressions for these indices are provided in the Appendix.

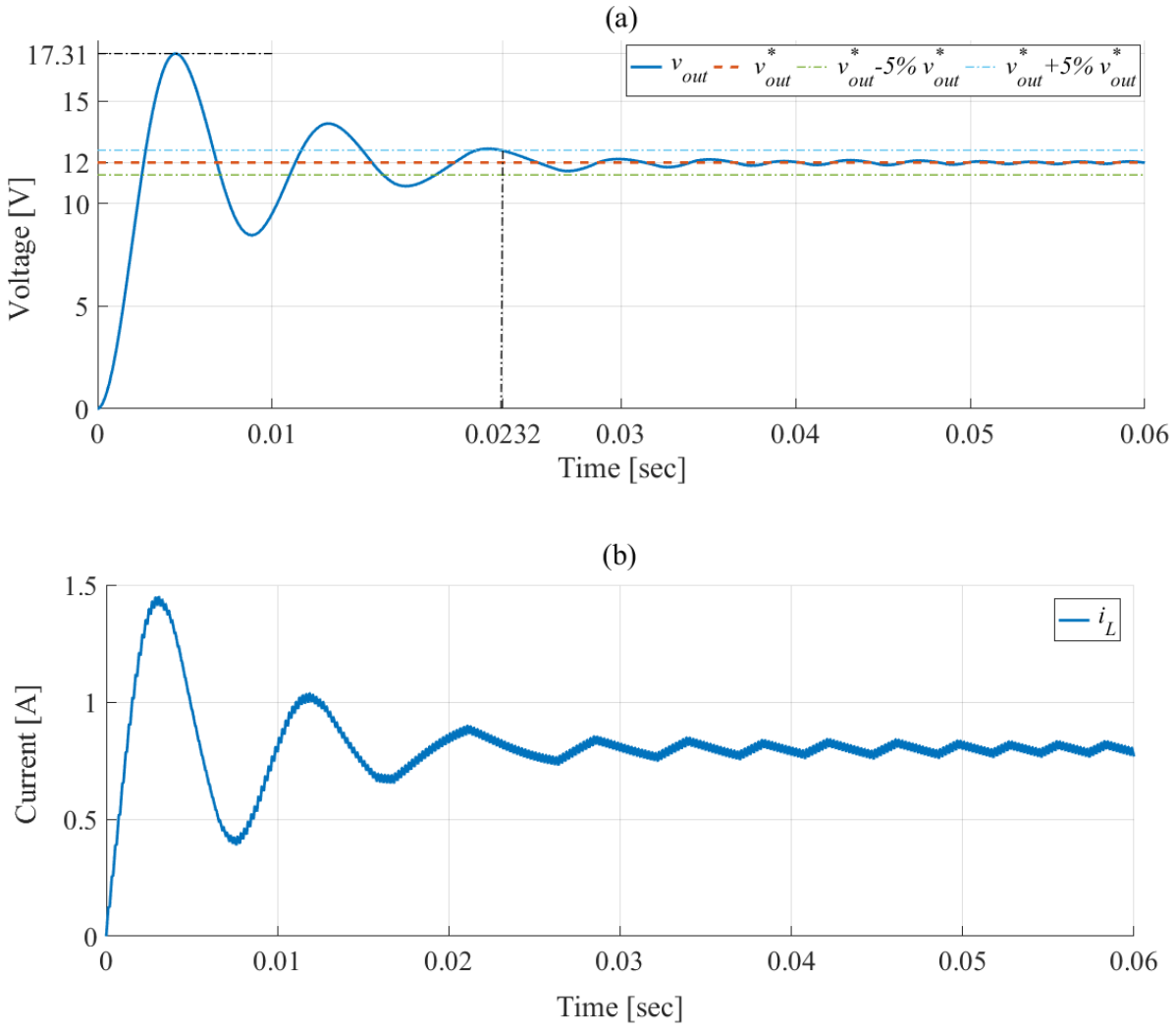

Figure I.11 . Simulation results of the Buck converter with PID controller under a fixed reference output voltage of 12 V: (a) output voltage, (b) inductor current.

Table I.10. Key performance metrics of the Buck converter using PID controller under a fixed reference output voltage of 12 V.

Controller	Settling Time [SEC]	Overshoot [V]	IAE	ISE	ITAE	ITSE
PID	0.0232	2.31	0.6	7.2	0.015	0.018

I.5. Conclusion

In this chapter, we investigated the modeling of static DC-DC converters, with a particular focus on the Buck converter, to facilitate the application and implementation of control techniques. A brief overview of various control methods for DC-DC converters was provided. Furthermore, the design of a PID controller for the Buck converter, along with its simulation results, was presented.

In the next chapter, we will focus on designing fuzzy controllers for the Buck converter to enhance the performance and robustness of the controlled system.

Chapter II:

Type 1 and Type 2 Fuzzy Logic Control

II.1. Introduction

Fuzzy control technique, as a branch of intelligent control, provides a valuable complement to traditional control methods by adopting a fundamentally different approach. It uses more information from domain experts and relies less on mathematical modeling. Since the mid-1980s, researchers have developed analytical structures for fuzzy controllers, particularly fuzzy PID controllers, ensuring guaranteed stability and specified performance. This progress has transformed fuzzy control from a heuristic technique into a rigorous and structured discipline, making it a safer, more efficient, and cost-effective solution for industrial applications [9].

In many studies related to power electronics systems [7], [10], [11], [12], [13], [14], fuzzy controllers have demonstrated their ability to improve robustness against parameter variations without the need for an exact model of the converter. They are a class of nonlinear adaptive control techniques, often outperforming traditional adaptive controllers in flexibility and ease of design. Motivated by these advantages, the present chapter focuses on the control of a buck converter using both Type-1 and Type-2 fuzzy logic control strategies.

II.2. Type-1 Fuzzy Logic Control

Type-1 fuzzy logic provides a mathematical framework for handling uncertainty by assigning degrees of membership between 0 and 1, rather than crisp, binary states. It uses fixed membership functions and a rule-based system (a set of *if-then* rules) derived from expert knowledge to map inputs to outputs. Type-1 fuzzy logic is well-suited for modeling complex, nonlinear systems without requiring an exact mathematical model. Its main advantages include intuitive design, robustness to noise, and effectiveness in poorly modeled or time-varying systems. However, its fixed membership functions limit adaptability under high uncertainty. In

control applications, type 1-fuzzy logic controller (T1-FLC) translate human expertise into control rules, offering a flexible and efficient alternative to traditional controllers [15].

II.2.1. Concept and Type-1 Fuzzy Set

Type-1 fuzzy logic systems model uncertainty using crisp membership functions that map inputs to values between 0 and 1. They enable rule-based reasoning in nonlinear or imprecise environments, effectively capturing the mean behavior of uncertain systems, analogous to the expected value in probability theory. However, type-1 systems cannot represent uncertainty within the membership functions themselves, limiting their ability to model variability. Despite this, they remain popular for their simplicity, interpretability, and efficiency, especially in applications with moderate uncertainty [3], [15].

II.2.1.1. Concept of Type-1 Fuzziness

Type-1 fuzzy sets, introduced by Lotfi Zadeh in 1965, generalize classical sets by assigning elements a degree of membership between 0 and 1, rather than a strict binary value. This allows for the modeling of imprecise or vague information using fixed membership functions, which define the degree of truth or inclusion of each element in a fuzzy set. Type-1 fuzzy logic systems operate using these predefined functions in conjunction with a rule-based structure, typically a collection of *if-then* rules derived from expert knowledge, to map inputs to outputs. This makes them particularly suitable for controlling complex, nonlinear systems without requiring an exact mathematical model [10].

II.2.1.2. Representation of a Type-1 Fuzzy Set

A Type-1 fuzzy set $\tilde{A}$ is represented by a membership function $\mu_{\tilde{A}}(x)$, which assigns each element x in the universe of discourse X a degree of membership between 0 and 1:

$$\tilde{A} = \{(x, \mu_{\tilde{A}}(x)) | x \in X\} \tag{II.1}$$

The $\mu_{\tilde{A}}(x)$ is a degree that indicates the extent to which x satisfies or belongs to a linguistic concept. The shape of the membership function commonly triangular, trapezoidal, or Gaussian defines how gradual or sharp the transition is between degrees of membership. Fuzzy sets enable partial membership, providing a more flexible and realistic representation of uncertain or vague concepts in real-world systems [16].

II.2.1.3. Types of Type-1 Fuzzy Sets

Type-1 fuzzy sets are classified according to the shape of their membership functions, such as triangular, trapezoidal, Gaussian, and sigmoidal. Triangular and trapezoidal types offered simplicity and low computational cost, while Gaussian and sigmoidal functions provided

smoother transitions for more precise modeling. Another important category is the singleton membership function, which assigns a full membership grade (typically 1) to a single value and zero elsewhere. Singletons are particularly useful in Takagi-Sugeno fuzzy systems, where they help produce crisp outputs efficiently [3].

The membership degrees for each of the aforementioned mentioned forms are presented in Figure II.1 and mathematically defined by the following expressions:

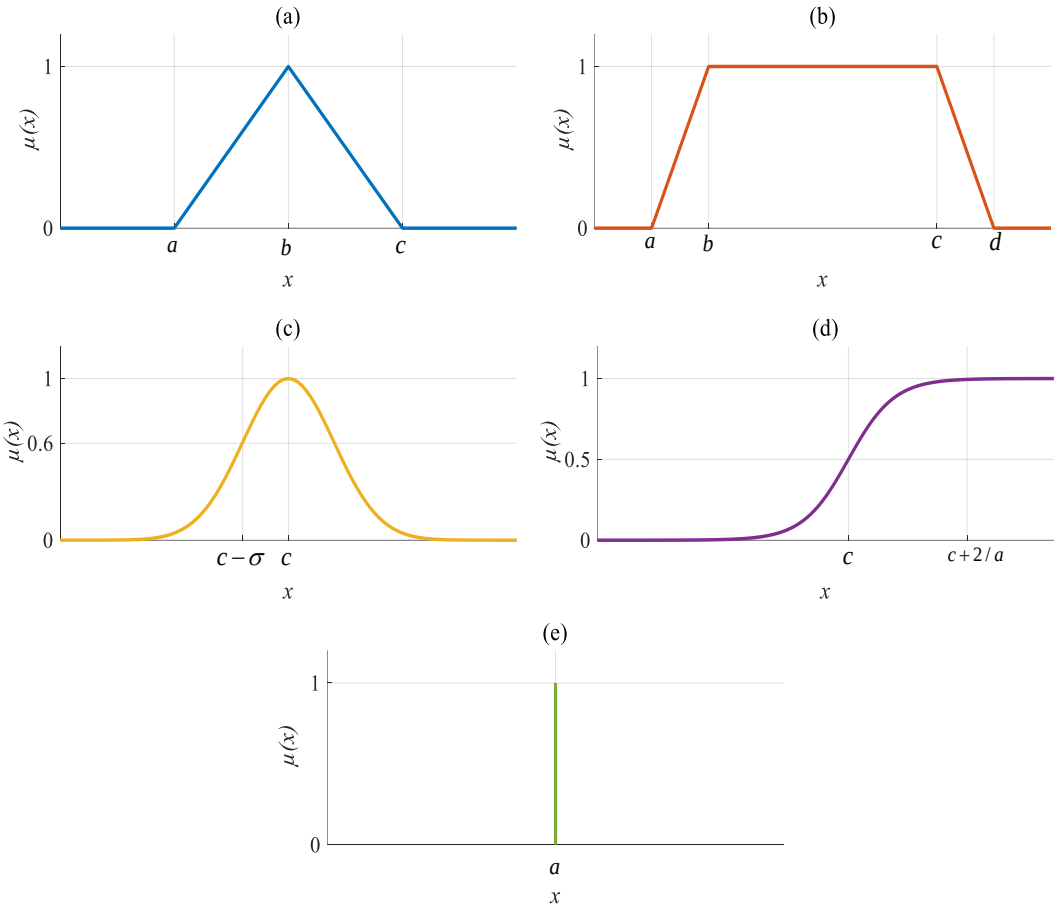

Figure II.1. Common shapes of membership functions of type-1 fuzzy sets: (a) Triangular, (b) Trapezoidal, (c) Gaussian, (d) Sigmoidal, and (e) Singleton.

- *Triangular*:

$$\mu(x) = \begin{cases} 0 & if\ x < a\ or\ x > c \\ \dfrac{x-a}{b-a} & if\ a \le x < b \\ \dfrac{c-x}{c-b} & if\ b \le x \le c \end{cases} \tag{II.2}$$

- *Trapezoidal*:

$$\mu(x) = \begin{cases} 0 & if\ x < a\ or\ x > d \\ \dfrac{x-a}{b-a} & if\ a \le x < b \\ 1 & if\ b \le x \le c \\ \dfrac{d-x}{d-c} & if\ c < x \le d \end{cases} \tag{II.3}$$

- *Gaussian*:

$$\mu(x) = e^{-\frac{(x-c)^2}{2\sigma^2}} \tag{II.4}$$

- *Sigmoidal*:

$$\mu(x) = \frac{1}{1 + e^{-a(x-c)}} \tag{II.5}$$

- *Singleton*:

$$\mu(x) = \begin{cases} 0 & if\ x \neq a \\ 1 & if\ x = a \end{cases} \tag{II.6}$$

The choice of membership function influenced system accuracy and interpretability, and was typically selected based on application-specific requirements.

II.2.2. Structure of a Type-1 Fuzzy Logic Controller

As depicted in Figure II.2, a type-1 fuzzy logic controller (T1-FLC) consists of four main components: fuzzification, inference engine, rule base, and defuzzification. It translates crisp inputs into fuzzy values, applies expert-defined *if-then* rules, and generates a crisp control output [4].

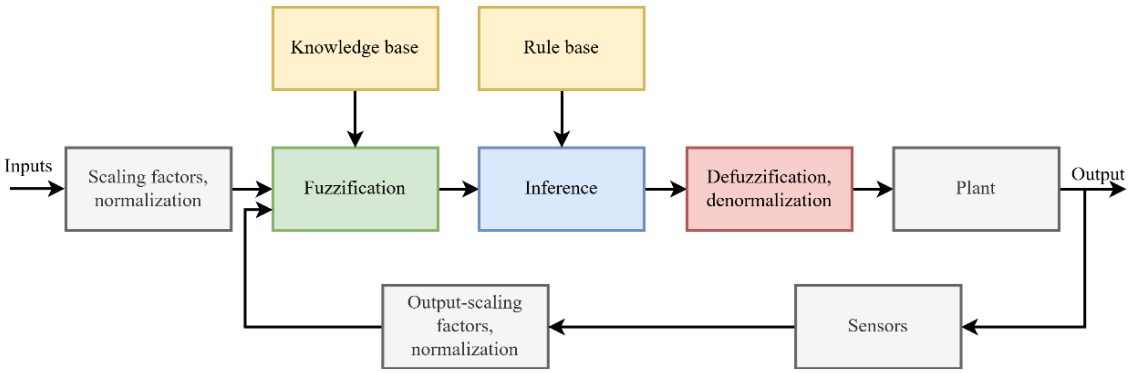

Figure II.2. General structure of the T1-FLC.

- *Fuzzifiation module*: This module is responsible for transforming crisp numerical input signals such as those generated by sensors into fuzzy values represented by linguistic variables. This conversion, often referred to as the "numerical-to-fuzzy" interface, maps physical quantities into fuzzy subsets defined over a specific universe of discourse. Each linguistic variable, defined through expert knowledge, must satisfy key criteria for effectiveness for example membership functions must maintain linguistic order. This process involves several core steps: receiving and scaling the input values to fit the normalized range, converting them into fuzzy sets using appropriate membership functions. Overall, the fuzzification module ensures that real-world inputs are accurately interpreted within the fuzzy control framework.

- *The knowledge base*: This module is the foundational core of T1-FLCs, composed of a data base and a linguistic rule base. The data base establishes the fuzzy sets, membership functions, scaling factors, and partitions of the input and output spaces. The rule base encodes expert knowledge or system models in the form of *if-then* rules, using linguistic variables to define control logic; each rule generates a fuzzy output, and the inference engine combines these using fuzzy operators. Aggregation is typically performed using a T-conorm function, such as the max operator:

$$\mu_A(x) = \max \mu_{Ai}(x) \mid i = 0,1, \dots, n \tag{II.7}$$

This step unifies all rule outputs into a single fuzzy set for defuzzification, enabling coherent decision-making in uncertain and nonlinear environments. Two prominent inference methods are:

i. Mamdani (Max-Min): Common in industrial control, it uses the "Min" operator for rule implication and the "Max" operator for aggregation. It is intuitive and effective for systems using linguistic outputs, such as error and its derivative.

ii. Sugeno (Sum-Product): Employing multiplication for rule firing strength and weighted averaging for output, it yields crisp functions or constants ideal for real-time and optimization-based applications.

Together, these mechanisms enable the T1-FLC to mimic expert reasoning, ensuring adaptability and robustness in complex control scenarios.

- *Defuzzification module*: This module serves as the final stage in a T1-FLC, converting the aggregated fuzzy output set into a crisp numerical value that can drive actuators or other physical systems. Often described as the "fuzzy-to-numerical" interface, the defuzzification process translates the result of fuzzy inference into a precise control action. It operates on the output fuzzy set and computes a single representative value, preserving system responsiveness and stability. Common defuzzification methods include the center of gravity, mean of maximum, height method, weighted average and weighted sum; the defuzzification module ensures seamless interaction between the fuzzy logic system and real-world actuation, enabling precise and effective control outputs. In our work (Takagi-Sugeno controller), the weighted average method is employed:

$$\Delta = \frac{\sum_{j=1}^{m} w_j \cdot c_j}{\sum_{j=1}^{m} w_j} \tag{II.8}$$

where w_j is the firing strength of the j^{th} rule, c_j is the crisp output (typically a constant or linear function), m is the total number of fuzzy rules.

Several structures of T1-FLCs have been developed in the literature. Table II.1 summarizes the main structures of fuzzy PID controllers [7]. These structures vary by input number (one, two, or three) and rule structure (coupled or decoupled). Coupled structures process all inputs in a single inference system, capturing complex interactions but increasing complexity. Decoupled structures use separate systems per input, simplifying design but potentially reducing precision. The choice depends on performance needs and system complexity.

Table II.1. Structures of Fuzzy PID Controllers.

Input's number	*Coupled rule structures*	*Decoupled rule structures*
Three inputs	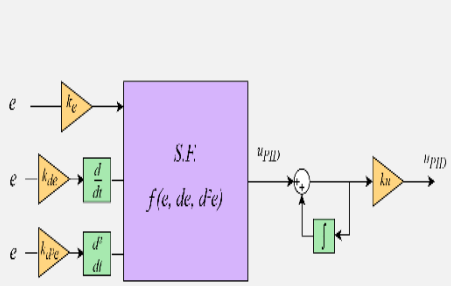	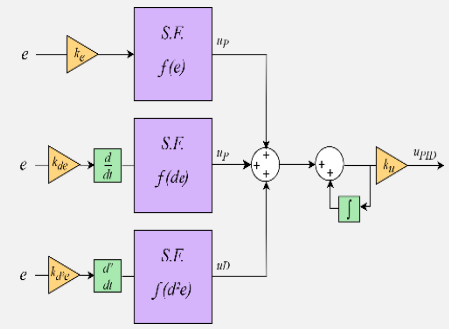
Two inputs	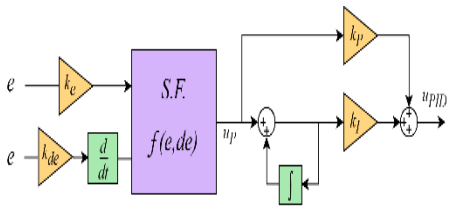	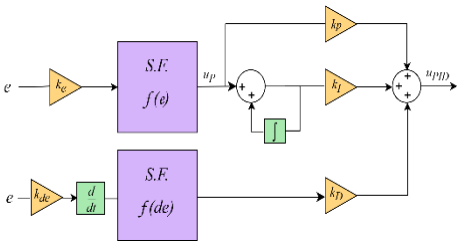
One input	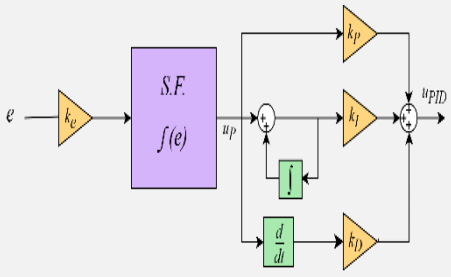	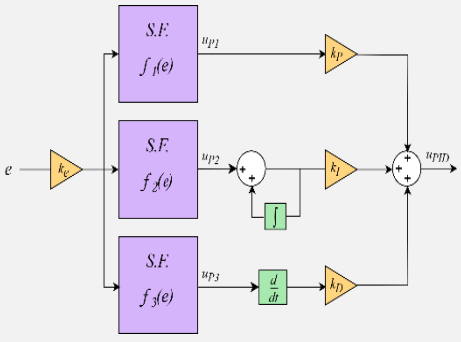

II.2.3. Design of a Type-1 Fuzzy Logic Controller for a Buck Converter

The structure of the designed T1-FLC for the Buck converter is schematized in Figure II.3, while its internal structure is detailed in Figure II.4. This structure is similar to that of a PI controller and was chosen for its simplicity, ease of implementation, and practical effectiveness.

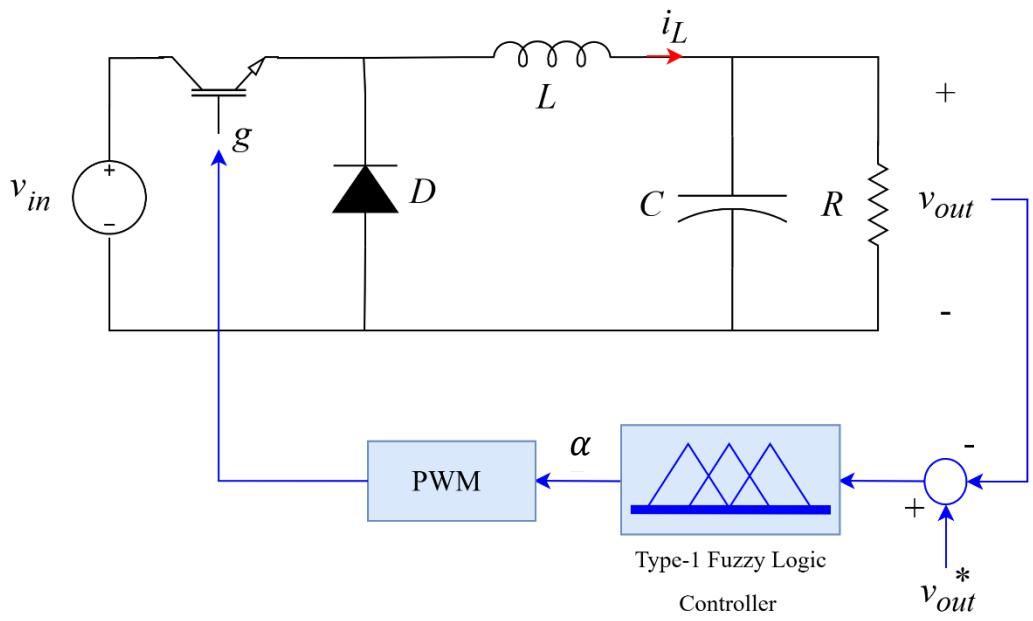

Figure II.3. Control scheme for the Buck converter using T1-FLC.

In this configuration, the input variables to the controller are the output voltage tracking error and its derivative, defined as:

$$e = k_e(v_{out}^* - v_{out}) \tag{II.9}$$

$$de = k_{de}\frac{d(v_{out}^* - v_{out})}{dt} \tag{II.10}$$

where k_e and k_{de} are normalizing coefficients for the controller inputs, and v_{out}^* represents the desired value for the Buck output voltage. The fuzzification process uses five non-symmetric triangular and trapezoidal membership functions for the input variables. To reduce computational complexity, a zero-order Takagi-Sugeno fuzzy model is selected for the controller, in which seven singleton fuzzy sets are used at the defuzzification stage. This choice enables faster computation and facilitates easier implementation in real-time systems. Both the input and output values are converted into an equal fuzzy range [−1, 1] to simplify the design complexity. The Min–Max algorithm is applied as the inference engine, which includes 25 *if–then* rules. All the membership functions and rules for the T1-FLC are illustrated in Figure II.4. The weighted average algorithm is used for the defuzzification and the output of the T1-FLC, i.e., the duty cycle α, is computed the following expression:

$$\alpha = k_p\Delta + k_i\int \Delta dt \tag{II.11}$$

where k_p is the de-normalizing proportional coefficient, k_i is the denormalizing integral coefficient, and u is the fuzzy controller output.

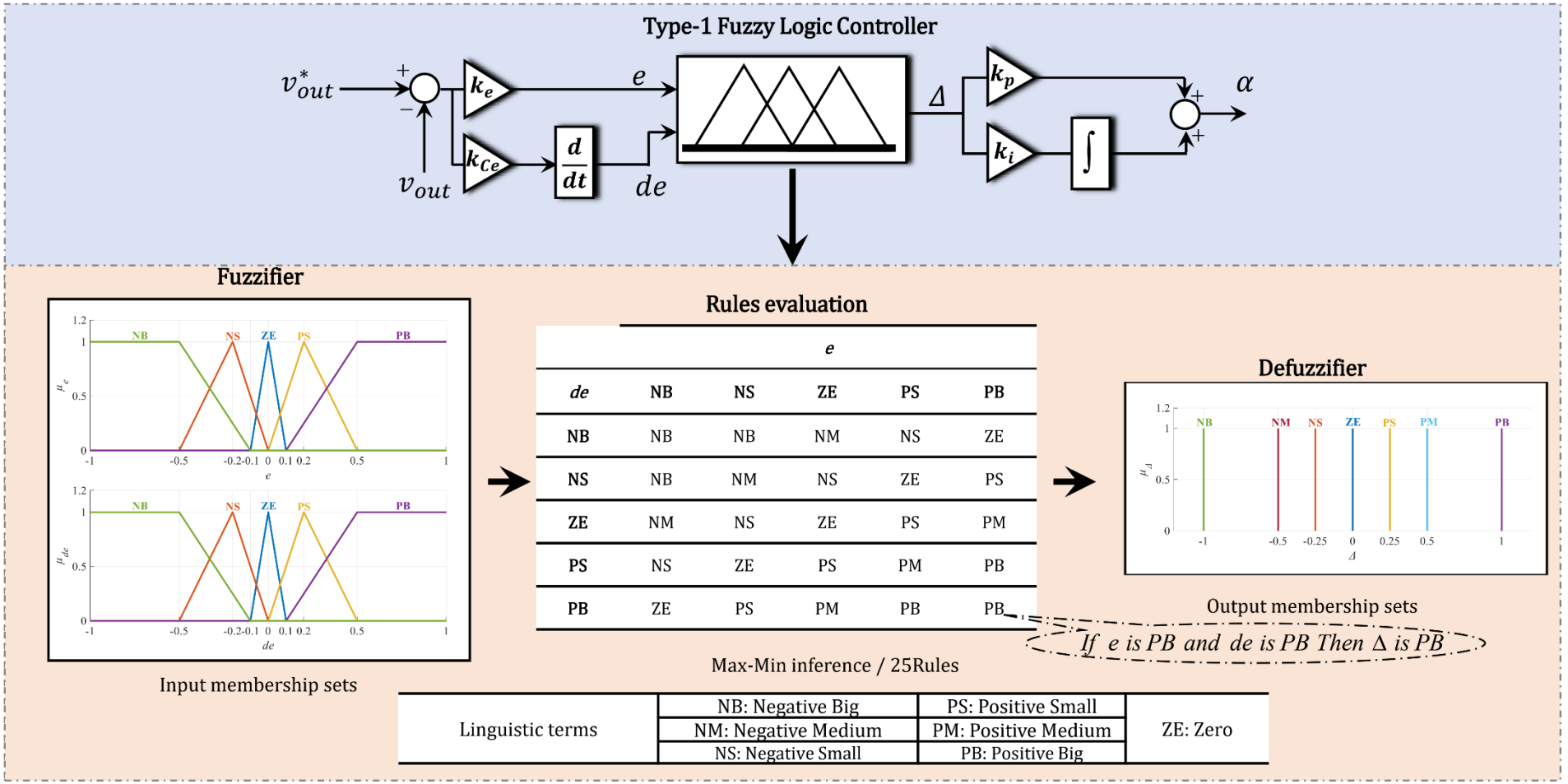

de \ *e*	NB	NS	ZE	PS	PB
NB	NB	NB	NM	NS	ZE
NS	NB	NM	NS	ZE	PS
ZE	NM	NS	ZE	PS	PM
PS	NS	ZE	PS	PM	PB
PB	ZE	PS	PM	PB	PB

Figure II.4. Designed structure of the T1-FLC.

II.2.4. Simulation results

For the simulation tests, the Type-1 Fuzzy Logic Toolbox of MATLAB®/Simulink® is used to implement and simulate the designed T1-FLC, in conjunction with the Simscape Power Systems package (formerly known as SimPowerSystems) to model the Buck converter. The T1-FLC simulates with a sample time of $0.1\ ms$. The coefficients $k_e = 0.1$, $k_{de} = 2.8$, $k_p = 5.3$ and $k_i = 1.6$ are manually tuned based on empirical observations obtained from the simulation results. The parameters of the Buck converter are the same as those used in Chapter I.

Figure II.5 shows the simulation results of the output voltage and the inductor current of the Buck converter controlled by the designed T1-FLC, under a fixed reference output voltage of 12 V. It can be observed that the output voltage tracks the reference voltage with reduced oscillations and a faster settling time compared to the system using PI control. The key performance parameters corresponding to these results are listed in Table II.2.

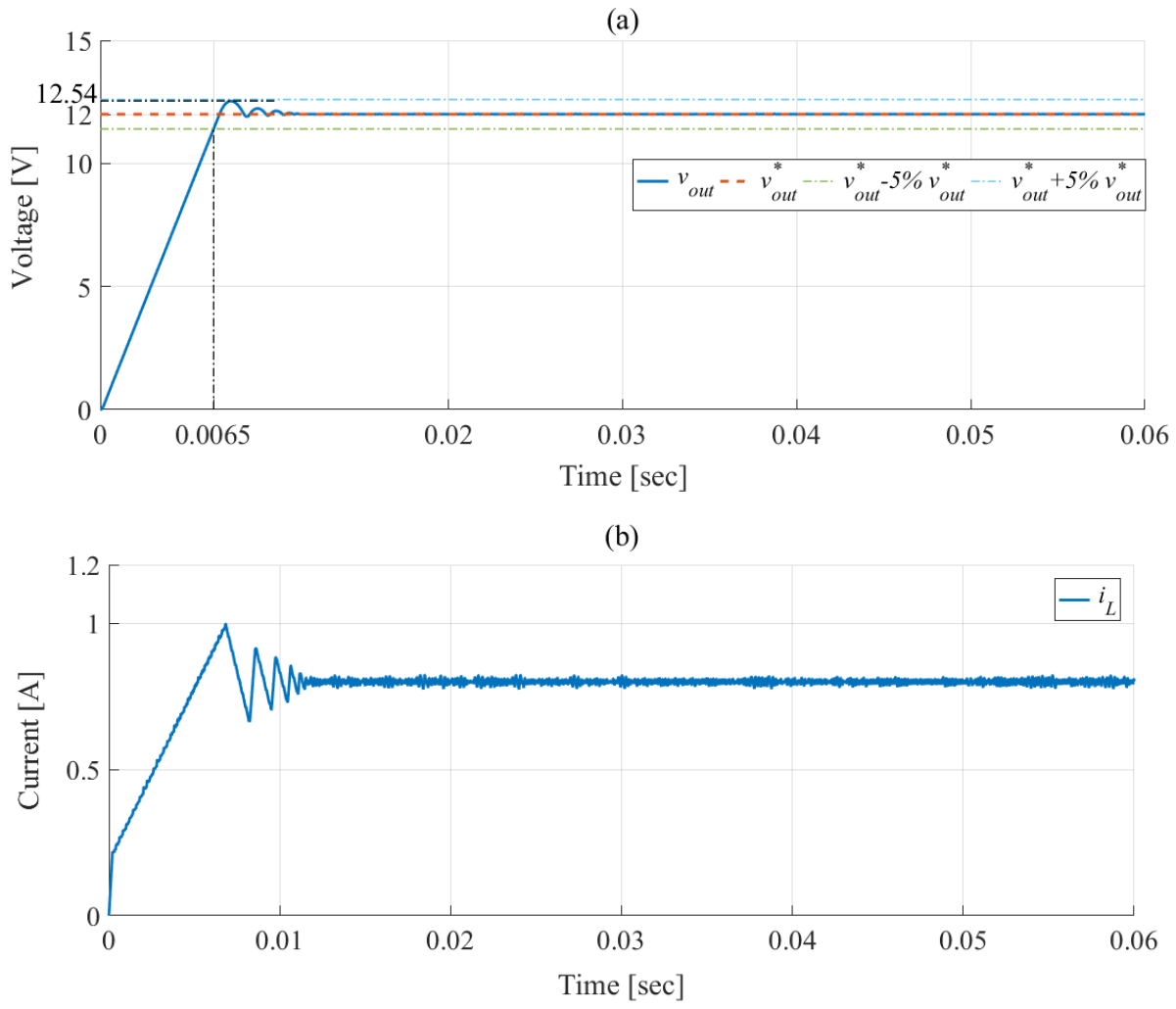

Figure II.5. Simulation results of the Buck converter with T1-FLC under a fixed reference output voltage of 12 V: (a) output voltage, (b) inductor current.

Table II.2. Key performance metrics of the Buck converter using T1-FLC under a fixed reference output voltage of 12 V.

Controller	Settling time [sec]	Overshoot [V]	IAE	ISE	ITAE	ITSE
T1-FLC	$6.51.10^{-3}$	0.54	0.04248	0.3385	0.0005812	0.0001032

II.3. Type-2 Fuzzy Logic Control

Type-2 fuzzy logic extends type-1 fuzzy systems by incorporating a secondary level of uncertainty, allowing membership grades to be fuzzy rather than crisp. This enhanced modeling capability makes type-2 fuzzy logic particularly effective in environments characterized by noise, ambiguity, and time-varying dynamics conditions where type-1 systems may struggle due to their fixed membership functions. By capturing uncertainty within the membership functions, type-2 fuzzy systems offer improved robustness and adaptability for complex, nonlinear systems. However, this comes at the cost of increased computational complexity. To address this, interval type-2 fuzzy systems are more commonly used, as they offer a good trade-off between accuracy and computational efficiency [17].

II.3.1. Concept and Type-2 Fuzzy Set

A type-2 fuzzy set extends the classical and type-1 fuzzy set concepts by allowing the membership grade itself to be fuzzy. This means that for each element in the universe of discourse, instead of assigning a precise membership value between 0 and 1 (as in type-1), a type-2 fuzzy set assigns a fuzzy set of membership values [18].

II.3.1.1. Concept of Type-2 Fuzziness

Type-2 fuzziness extends the concept of uncertainty modeling by not only allowing partial membership in a set, but also enabling uncertainty within the membership grades themselves. Unlike type-1 fuzzy sets, where membership values are precise numbers between 0 and 1, type-2 fuzzy sets assign a range of possible membership values, represented by a fuzzy set. This additional dimension allows type-2 fuzzy logic to better handle real-world scenarios involving noisy measurements, ambiguous linguistic terms, and expert disagreement. It is especially useful in complex systems where uncertainties are not only present in the data but also in how that data is interpreted [17].

II.3.1.2. Representation of a Type-2 Fuzzy Set

Formally, let X be the universe of discourse. A type-2 fuzzy set $\tilde{A}$ in X is defined as a set of ordered triples:

$$\tilde{A} = \{(x, u, \mu_{\tilde{A}}(x, u)) | x \epsilon X, u \epsilon J_x \subseteq [0\,, 1]\} \quad \text{(II.12)}$$

where x is an element of the universal set X, u is a secondary membership value from the primary membership domain J_x, $\mu_{\tilde{A}}(x, u) \in [0\,,\ 1]$ is the secondary membership function, representing the degree of confidence or possibility that u is the true membership grade of x.

This contrasts with a type-1 fuzzy set, where the membership function $\mu_{\tilde{A}}(x)$ is a single-valued mapping $X \rightarrow [0\,, 1]$. In a Type-2 fuzzy set, the primary membership function maps each input x to a fuzzy set over the unit interval, resulting in a three-dimensional membership surface.

When all secondary grades $\mu_{\tilde{A}}(x, u)$ are equal to 1 (i.e., all values in the footprint of uncertainty (FOU) are equally possible), the type-2 fuzzy set simplifies to an interval type-2 fuzzy set, where uncertainty is represented by a bounded region (FOU) between an upper membership function (UMF) and a lower membership function (LMF), as illustrated in Figure II.6. This structure allows Type-2 fuzzy sets to model uncertainty in the membership grades themselves, accommodating ambiguity from linguistic terms, sensor noise, and expert disagreement.

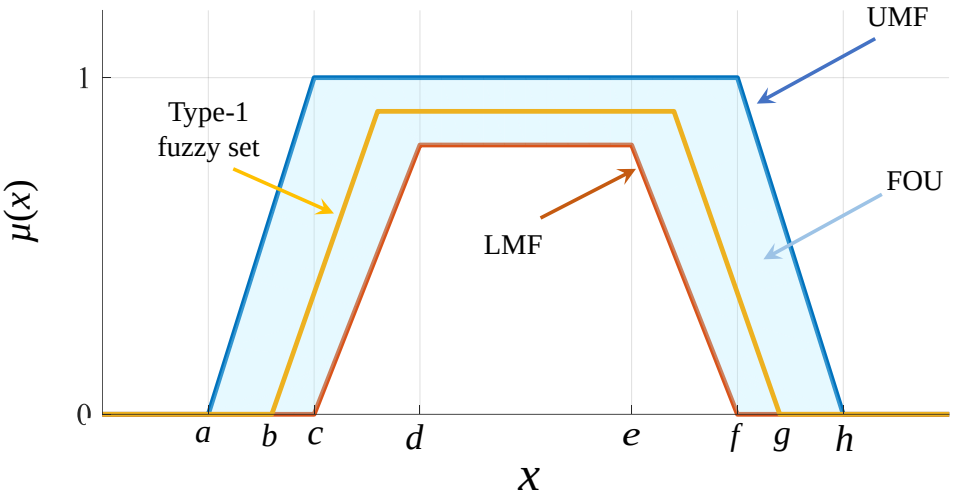

Figure II.6. Membership function of the interval type-2 fuzzy set.

II.3.1.3. Types of Type-2 Fuzzy Sets

Type-2 fuzzy sets are categorized based on the structure of their upper and lower membership functions. In Gaussian and triangular type-2 sets for example, each point's membership is defined by a type-1 Gaussian or triangular fuzzy set over [0 , 1]. In interval type-2 sets, all secondary grades are equal to 1, and uncertainty is captured by the upper and lower membership functions forming the FOU. Figure II.7 shows examples of fuzzy interval type-2 sets.

The choice between interval type-2 fuzzy sets, and between membership shapes like Gaussian or trapezoidal, depends on the desired balance between modeling precision and computational efficiency.

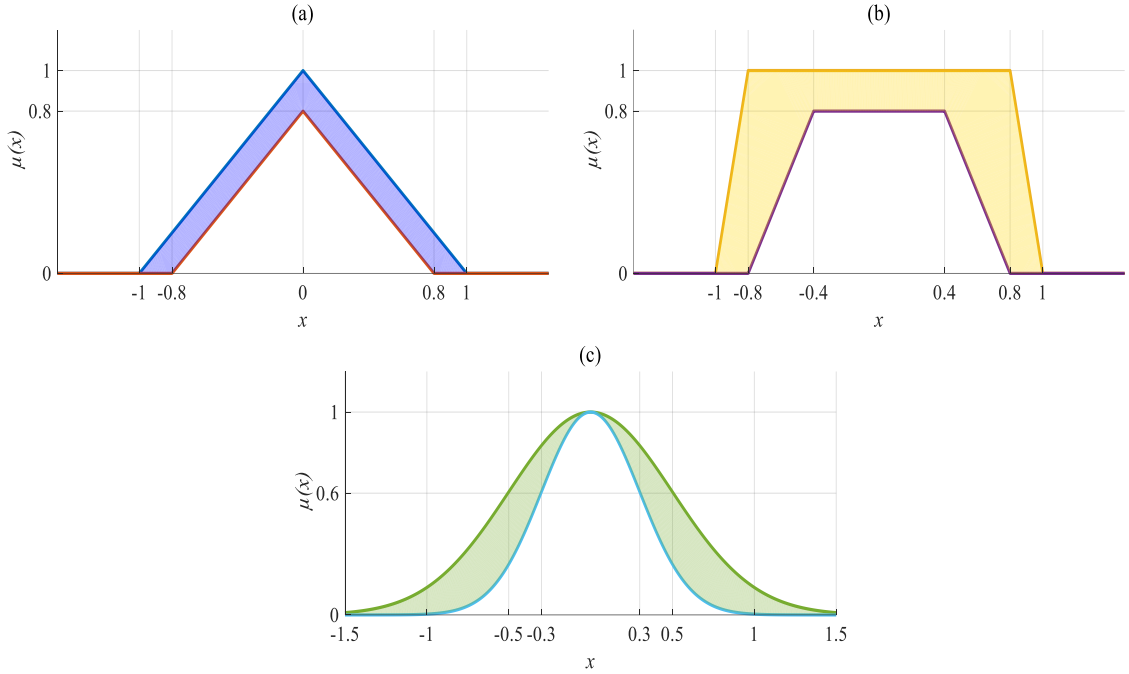

Figure II.7. Examples of interval type-2 fuzzy sets: (a) Triangular, (b) Trapezoidal, and (c) Gaussian.

II.3.2. Structure of a Type-2 Fuzzy Logic Controller

The architecture of a type-2 fuzzy logic controller (T2-FLC) mirrors the structure of a T1-FLC, but adds a crucial type-reduction stage, as shown in Figure II.8.

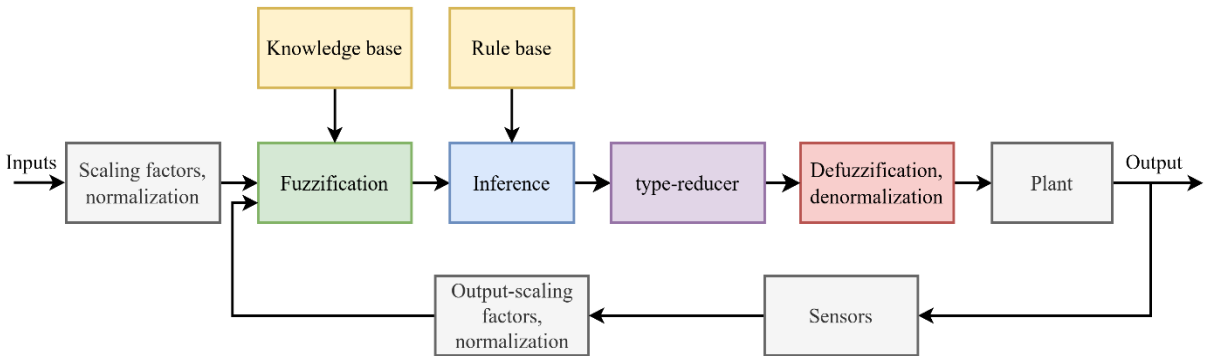

Figure II.8. General structure of the T2-FLC.

The T2-FLC includes five main components: fuzzification, inference engine, rule base, type-reduction, and defuzzification, described as follows:

- *Fuzzification module*: This stage transforms crisp numerical input signals into fuzzy linguistic variables characterized by type-2 fuzzy sets. Unlike type-1 systems, where each value maps to a fixed membership grade, type-2 fuzzification assigns a fuzzy set

of membership grades to each input, forming a FOU. This process enables the system to model uncertainty directly within the membership functions. Inputs are first normalized to fit within a defined universe of discourse and then mapped using primary membership functions, each bounded by upper and lower curves to reflect ambiguity. This module ensures accurate and uncertainty-aware interpretation of real-world signals within the type-2 fuzzy control framework.

- *Knowledge base*: The knowledge base of a T2-FLC includes both a data base and a rule base. The data base defines the type-2 fuzzy sets for all input and output variables, including the structure of their FOUs and associated scaling factors. The rule base contains *if-then* rules constructed from expert knowledge or modeling insights, using type-2 linguistic variables to express both premises and consequents. The inference engine evaluates these rules by processing secondary membership grades, producing type-2 fuzzy outputs. Aggregation of fuzzy outputs across all rules is typically achieved using a T-conorm same as type 1 aggregation.

- *Type reducer*: In type-2 fuzzy logic systems, the inference output is a type-2 fuzzy set, which must first undergo type-reduction before defuzzification. The Karnik-Mendel algorithm is commonly used to perform this task, offering a reliable balance between computational efficiency and accuracy. The Karnik-Mendel algorithm iteratively computes the left and right bounds y_l and y_r of the type-reduced interval by weighting rule consequents according to their firing strengths. The final crisp output Y_{KM} is typically the average of these bounds:

$$Y_{KM}(Y_1, \dots, Y_k, F_1, \dots, F_k) = [y_l, y_r\ ] \tag{II.13}$$

here, y_l and y_r are the left and right bounds of the type-reduced set, computed as weighted averages of the rule outputs $Y_j = [y_{jl}, y_{jr}\ ]$, based on their respective firing strengths F_j . This process captures the uncertainty from both the fuzzy rule consequents and their activation levels. This approach preserves the uncertainty encoded in the fuzzy output while producing a type-1 set suitable for defuzzification.

- *Defuzzification module*: This module converts the interval-valued set into a crisp control output suitable for actuation. This transformation, often referred to as the "fuzzy-to-crisp" interface, is crucial for producing precise, real-world control actions. In Interval type-2 systems, the most commonly used defuzzification method is the centroid of the type-reduced set, calculated as:

$$y(x) = \frac{y_l + y_r}{2} \tag{II.14}$$

This approach provides a representative scalar value that balances system responsiveness with uncertainty tolerance. In Takagi-Sugeno T2-FLCs, the defuzzification stage completes the reasoning cycle by producing a crisp output that captures both the logical structure of the rule base and the uncertainty modeled throughout the inference process.

II.3.3. Design of a Type-2 Fuzzy Logic Controller for a Buck Converter

Figure II.9 illustrates the structure of the designed T2-FLC for the Buck converter, while its internal structure is detailed in Figure II.10.

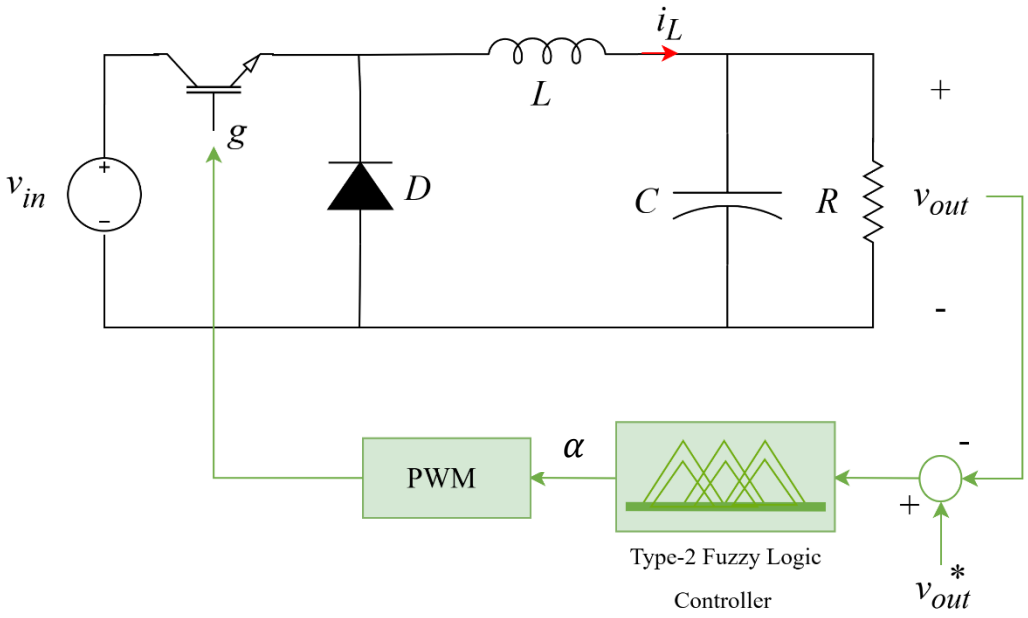

Figure II.9. Control scheme for the Buck converter using T2-FLC.

It can be observed that the T2-FLC inputs are the same as those used by the T1-FLC. The input signals are fuzzified using five interval Type-2 fuzzy sets with triangular and trapezoidal membership functions, as shown in Figure II.10. In addition, as fuzzifier output, seven singleton fuzzy sets are used. To simplify the design complexity, both the input and output variables are normalized to the fuzzy range [−1, 1]. The T2-FLC requires 25 fuzzy control rules; these rules are exactly the same as those of the T1-FLC. All the rules for the T2-FLC are also shown in Figure II.10. To activate the fuzzy rules, the Max–Min method is used as the inference engine. The defuzzification process is the last stage in implementing the T2-FLC, where the center-weighted average algorithm is used to trans-form the reduced fuzzy sets of the output into crisp value. Many types of reduction algorithm have been applied for T2-FLC. In this work, an appropriate reducer algorithm, Karnik–Mendel, is chosen.

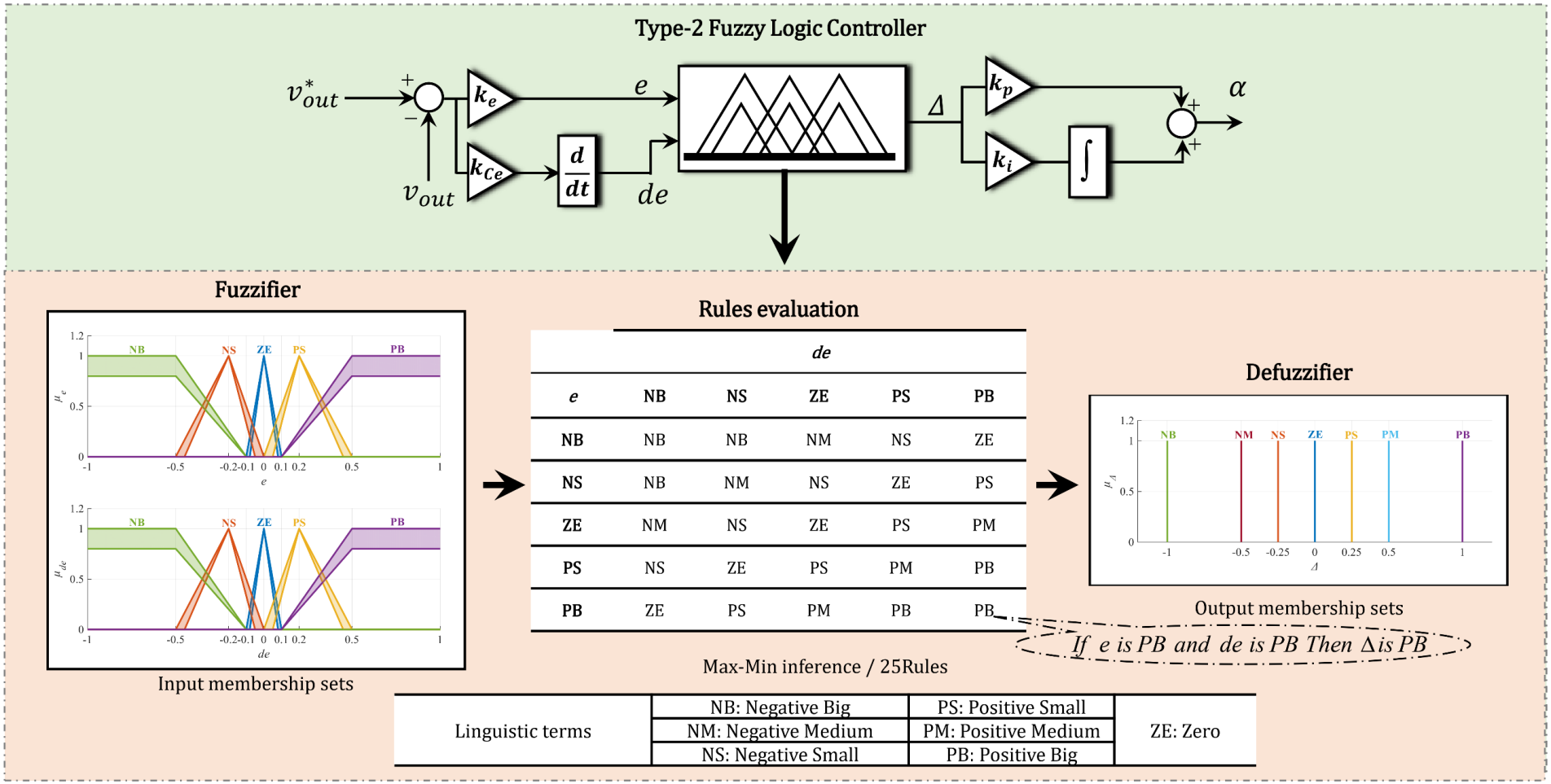

e \ de	NB	NS	ZE	PS	PB
NB	NB	NB	NM	NS	ZE
NS	NB	NM	NS	ZE	PS
ZE	NM	NS	ZE	PS	PM
PS	NS	ZE	PS	PM	PB
PB	ZE	PS	PM	PB	PB

Linguistic terms			
	NB: Negative Big	PS: Positive Small	ZE: Zero
	NM: Negative Medium	PM: Positive Medium	
	NS: Negative Small	PB: Positive Big	

Figure II.10. Designed structure of the T2-FLC.

II.3.4. Simulation results

Similarly, for the Type-2 controller, the T2-FLC Toolbox of MATLAB®/ Simulink® is used to implement and simulate the designed T2-FLC, in conjunction with the Simscape Power Systems package (formerly known as SimPowerSystems) to model the Buck converter. The T2-FLC simulates using the same sample time of 0.1 ms. The coefficients $k_e = 0.1$, $k_{de} = 2.5$, $k_p = 5.35$ and $k_i = 1.8$ are maintained for consistency. The Buck converter parameters remain unchanged from those used in Chapter I.

Figure II.11 displays the simulation results of the output voltage and the inductor current of the Buck converter controlled by the designed T2-FLC, under a fixed reference output voltage of 12 V. It can be noted that the output voltage tracks perfectly the reference voltage with minimal steady-state error and a faster settling time compared to the system using T2-FLC. Table II.3 summarizes the key performance parameters corresponding to these results. A more detailed comparison between the designed controllers will be presented in the following section.

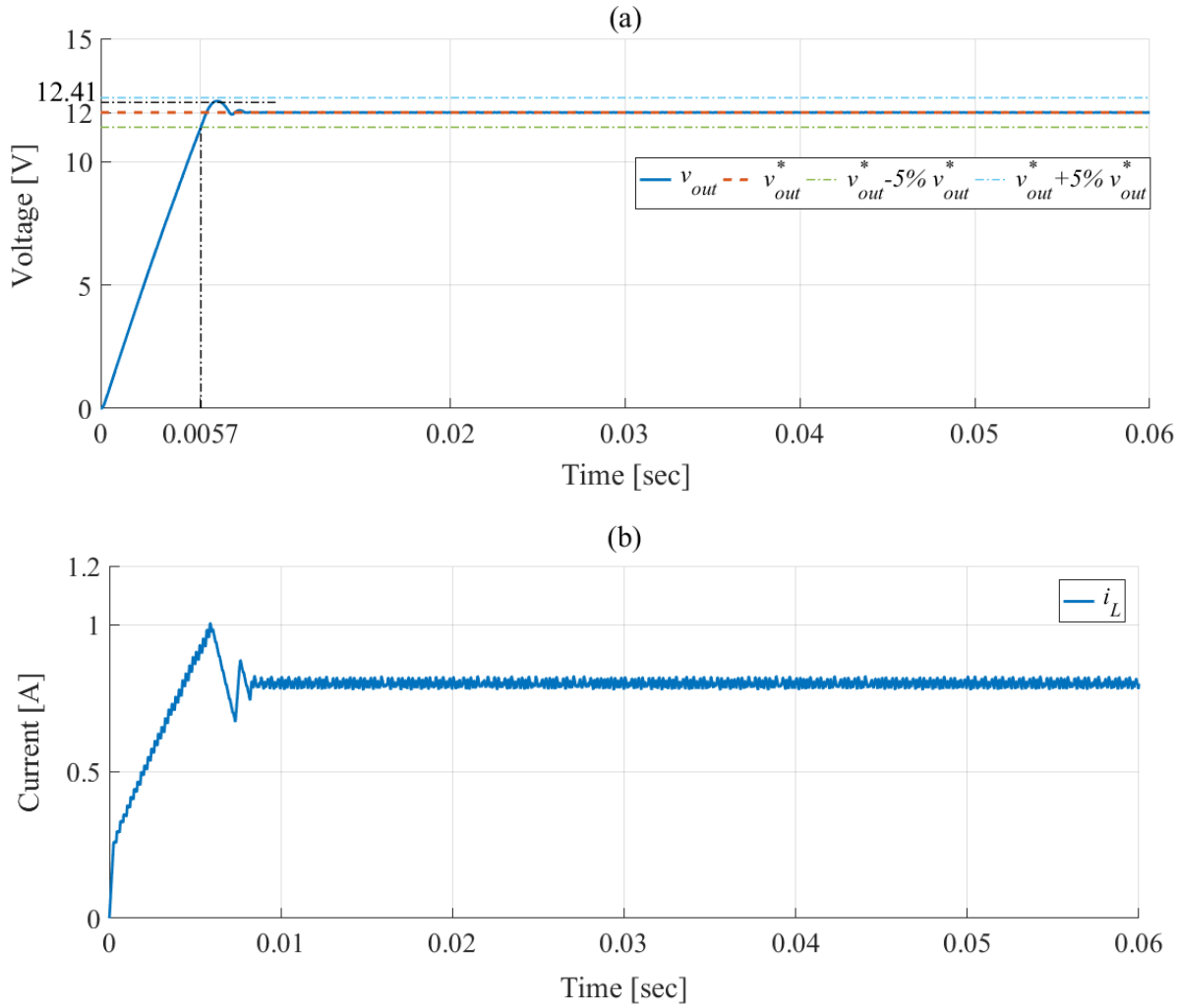

Figure II.11. Simulation results of the Buck converter with T2-FLC under a fixed reference output voltage of 12V: (a) output voltage, (b) inductor current.

Table II.3. Key performance metrics of the Buck converter using T2-FLC under a fixed reference output voltage of 12 V.

Controller	Settling time [sec]	Overshoot [V]	IAE	ISE	ITAE	ITSE
T2-FLC	$5.73.10^{-3}$	0.41	0.03664	0.2911	$8.061.10^{-5}$	0.0004294

II.5. Comparative study

To evaluate the effectiveness and robustness of the designed controllers, a comparative study is conducted between the classical PI controller, the T1-FLC, and the more advanced T2-FLC applied to a Buck converter under various operating scenarios.

II.5.1. Performance Comparison under Output Voltage Reference Tracking

First, a comparison of the different controllers under step changes in the output voltage reference is presented in Figure II.12.

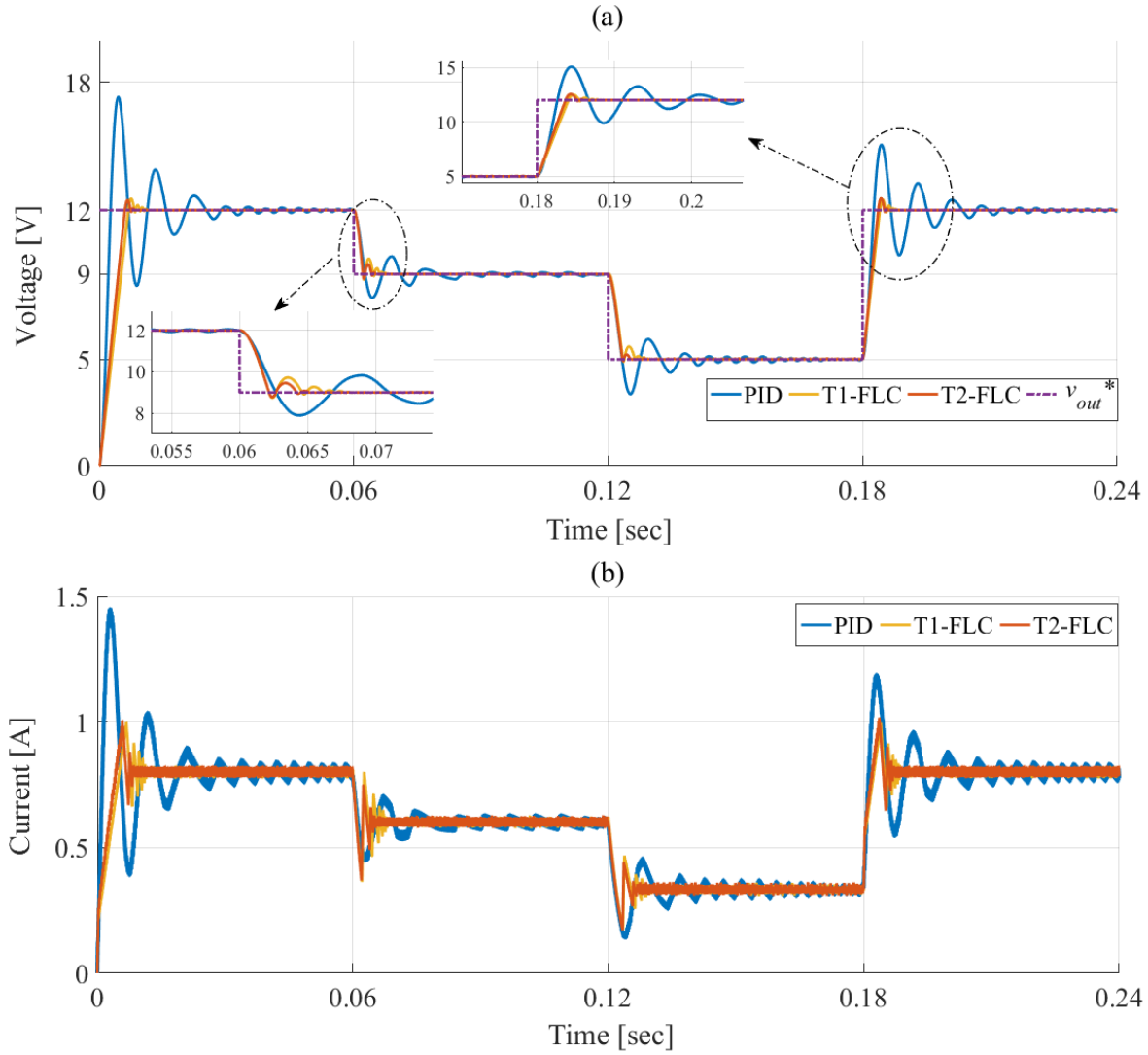

Figure II.12. Simulation results of the Buck converter with different controllers under step changes in the output voltage reference: (a) output voltage, (b) inductor current.

The step response characteristics of the different controllers, summarized in Table II.4, indicate that all controllers achieved good tracking performance in the steady state. However, in the transient state, the output voltage of the Buck converter showed a shorter settling time and smaller overshoot/undershoot when controlled by the fuzzy controllers (Type-1 and Type-2), with a slight advantage observed for the T2-FLC in terms of dynamic response.

Table II.4. Quantitative comparison of the three controllers under step changes in in the output voltage reference.

	Step increase in the output voltage 0 →12		**Step decrease in the output voltage 12 →9**		**Step decrease in the output voltage 9 → 5**		**Step increase in the output voltage 5→12**	
	Settling time [sec]	**Overshoot [V]**	**Settling time [sec]**	**Undershoot [V]**	**Settling time [sec]**	**Undershoot [V]**	**Settling time [sec]**	**Overshoot [V]**
PID	0.02312	5.31	0.2426	1.7489	0.08909	1.69502	0.17089	3.0872
T1FLC	$6.51 \cdot 10^{-3}$	0.54	0.2287	0.25094	0.07917	0.10698	0.15579	0.5185
T2FLC	$5.73 \cdot 10^{-3}$	0.41	0.2284	0.21065	0.07691	0.06126	0.15313	0.6417

In addition, Figures II.13 and II.14 illustrate a comparison of the different controllers under sinusoidal and triangular reference voltage tracking, respectively. It can be observed that the T2-FLC provides faster transient response and better steady-state performance in tracking the output voltage compared to the T1-FLC. Meanwhile, the PI controller fails to accurately follow the output voltage reference under these dynamic conditions.

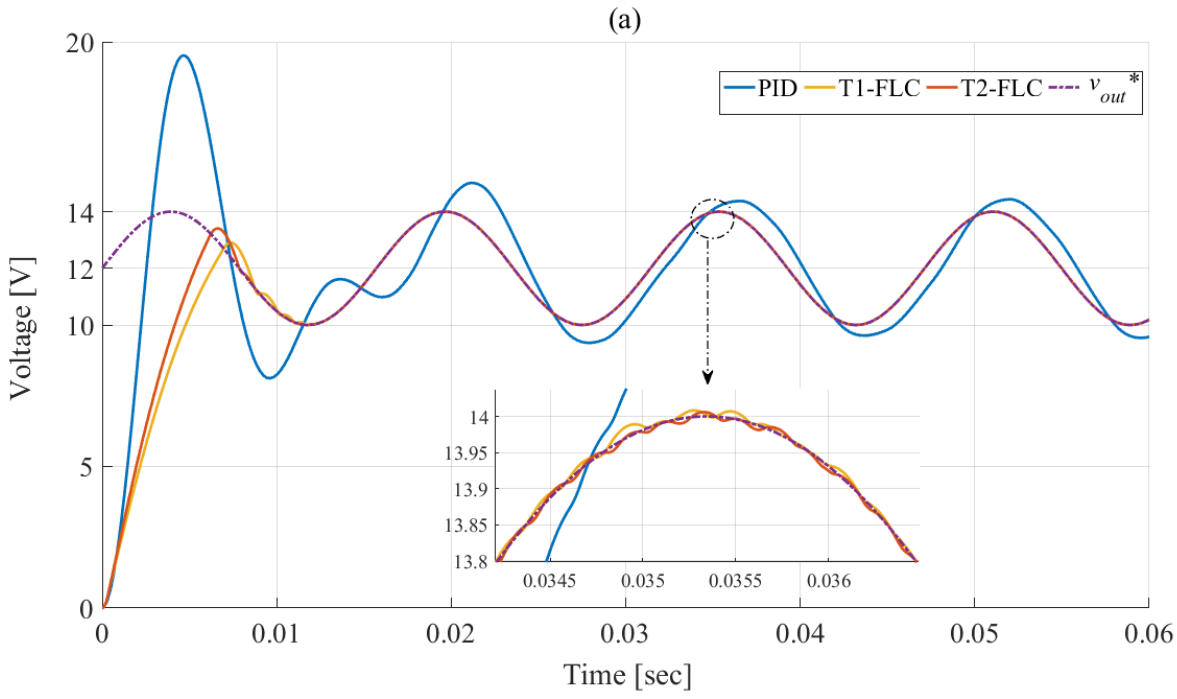

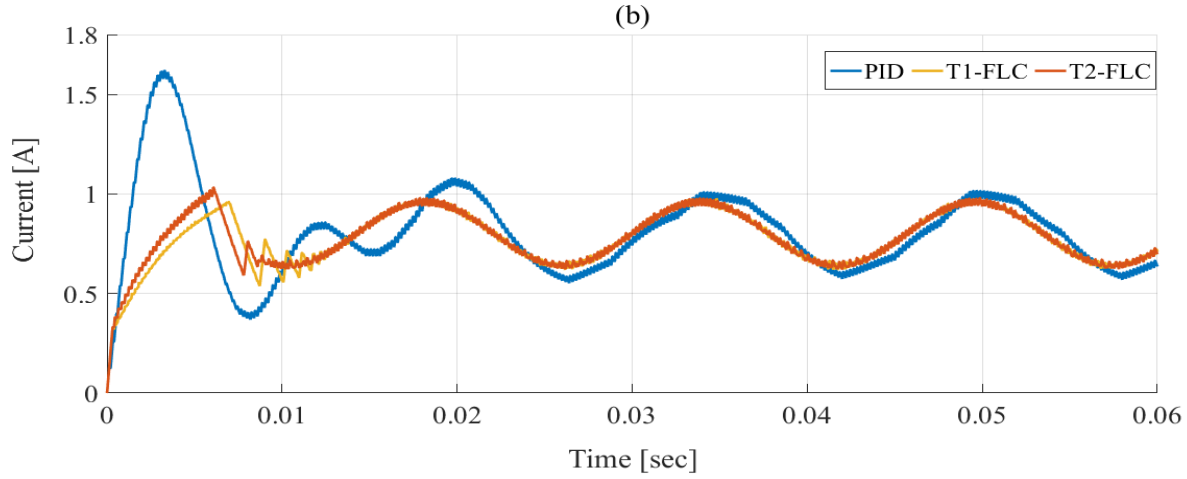

Figure II.13. Simulation results of the Buck converter with different controllers under sinusoidal-wave tracking: (a) output voltage, (b) inductor current.

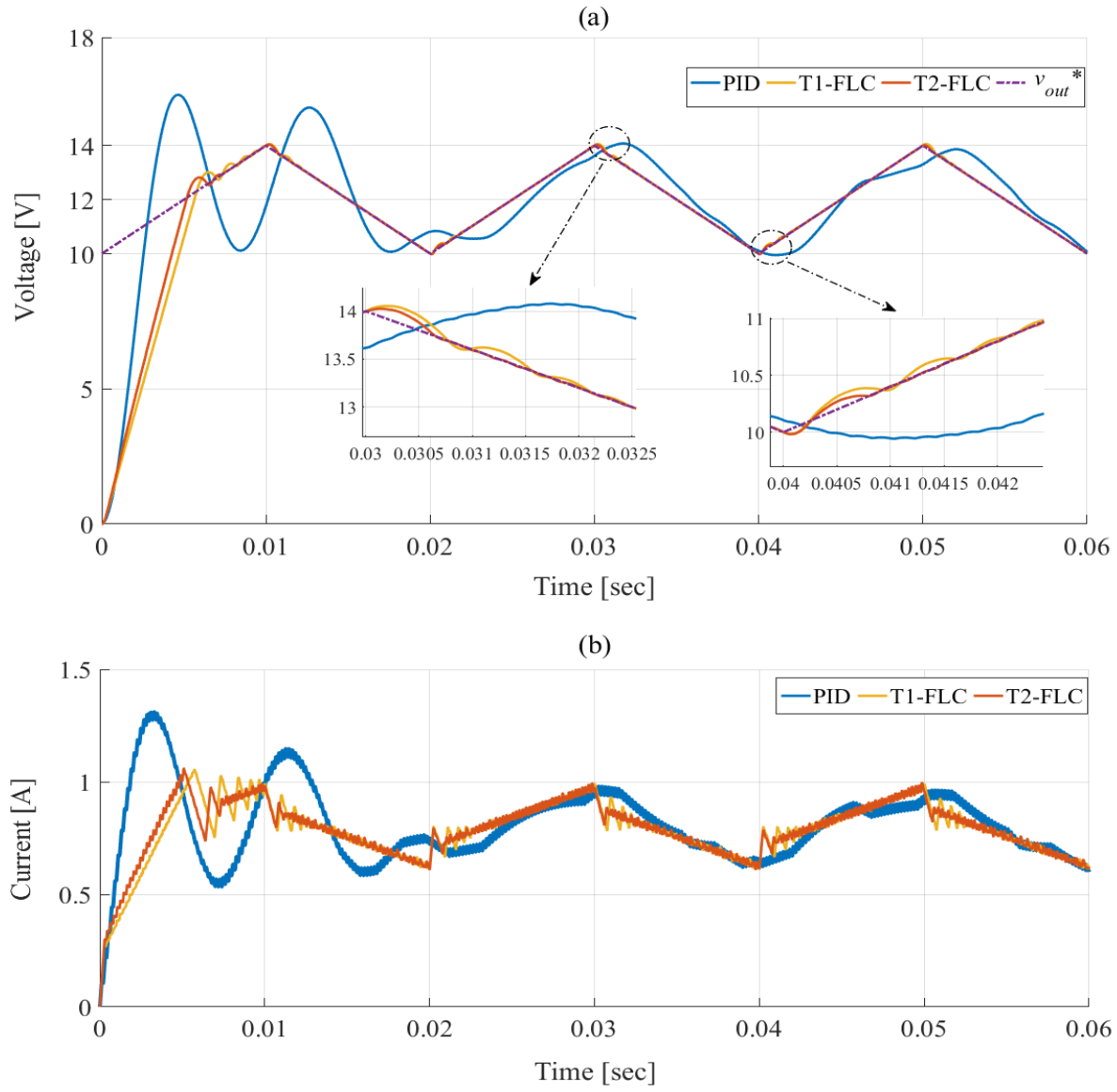

Figure II.14. Simulation results of the Buck converter with different controllers under triangular-wave tracking: (a) output voltage, (b) inductor current.

II.4.2. Performance Comparison under Load Variations

In this test, the three controllers were evaluated and compared under abrupt changes in the resistive load, specifically from 15 Ω to 7.5 Ω and then back to 15 Ω while maintaining a fixed output voltage reference of 12 V. Figure II.15 illustrates the ability of each controller to maintain to regulate the output voltage at 12 V despite these sudden variations in load. It can be seen from simulation results showed in Figure II.14 and Table II.5 that the output voltage responses of the three controllers became stable again after short transient. Nevertheless, the output voltage with the T2-FLC is faster and smaller overshoot/undershoot, demonstrating its superior disturbance rejection capability.

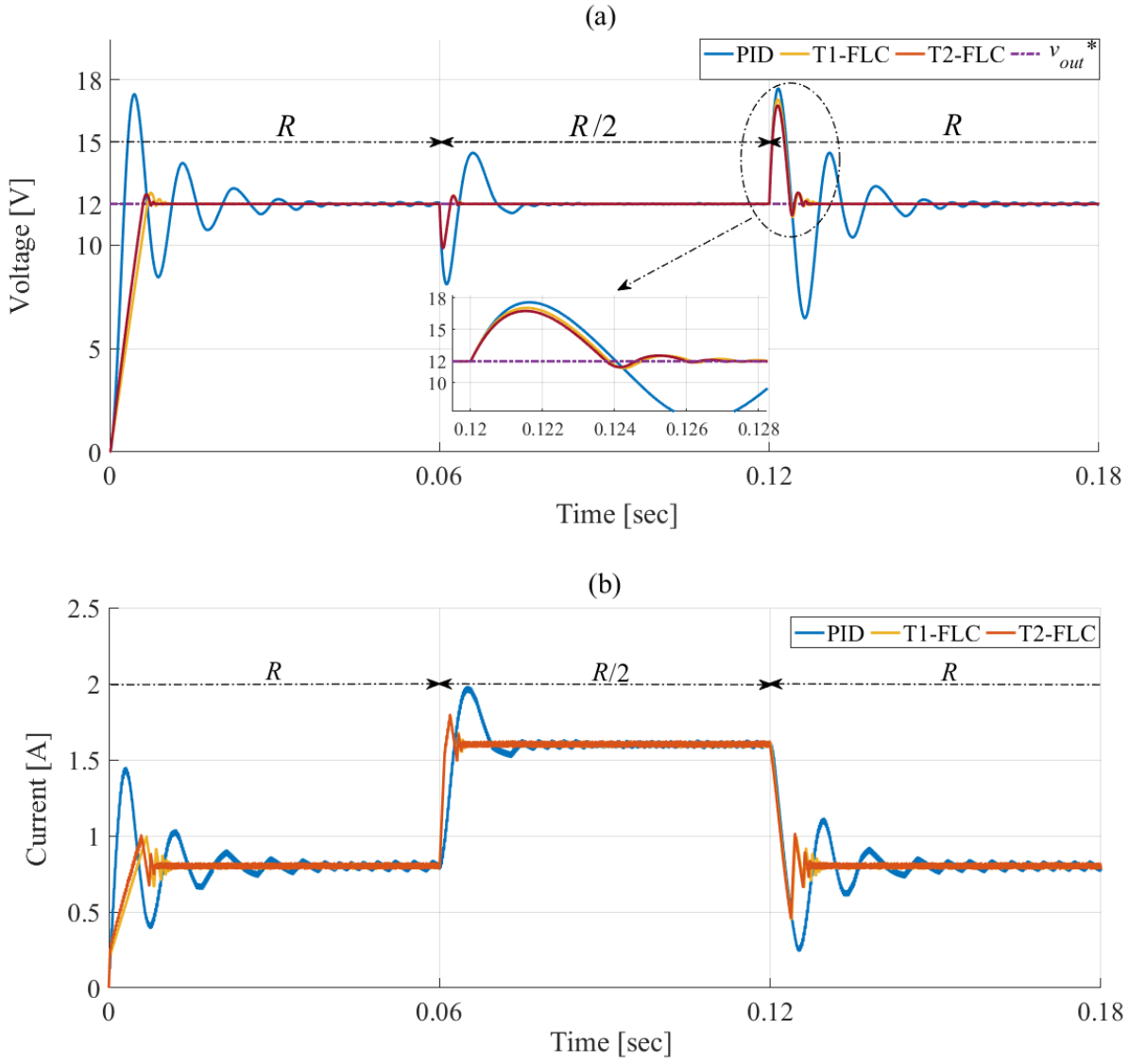

Figure II.15. Simulation results of the Buck converter with different controllers under step changes in the resistive load : (a) output voltage, (b) inductor current.

Table II.5. Quantitative comparison of the three controllers under step changes in the resistive load.

	Step decrease in the load $R \rightarrow R/2$		**Step increase in the load $R/2 \rightarrow R$**	
	Settling time [sec]	**Undershoot [V]**	**Settling time [sec]**	**Overshoot [V]**
PID	0.07447	3.885	0.14631	5.5824
T1-FLC	0.06297	2.0969	0.12692	4.9767
T2-FLC	0.06288	2.1577	0.12579	4.7883

II4.3. Performance Comparison under Input Voltage Disturbances

In this test, the Buck converter is tested under varying input voltage conditions. A composite voltage profile, comprising linear ramps, sinusoidal waves, and sawtooth waveforms, is applied to the converter to simulate dynamic and non-ideal supply conditions. This test aims to evaluate the robustness of the three controllers and their ability to maintain a regulated output voltage of 12 V despite disturbances in the input voltage.

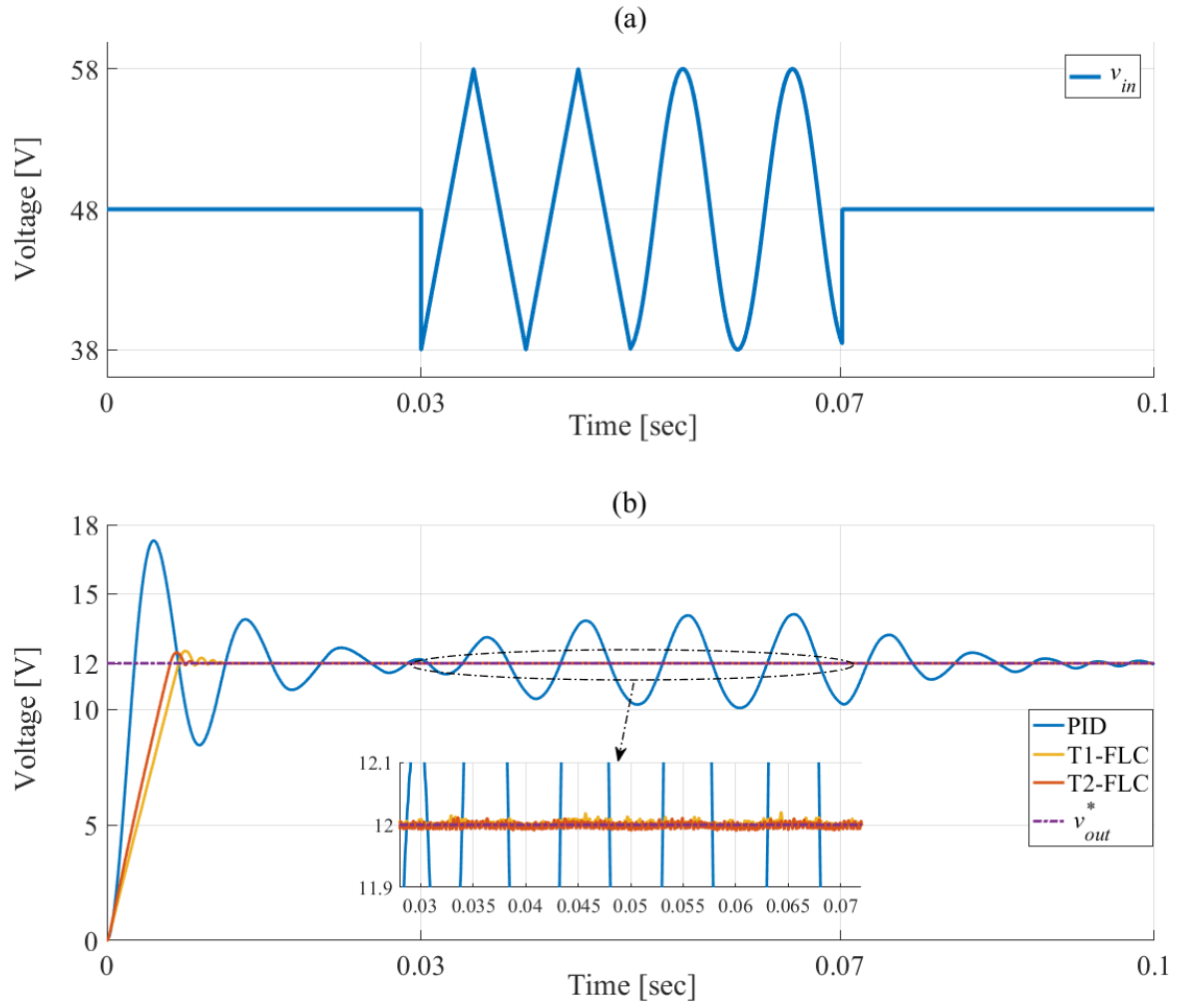

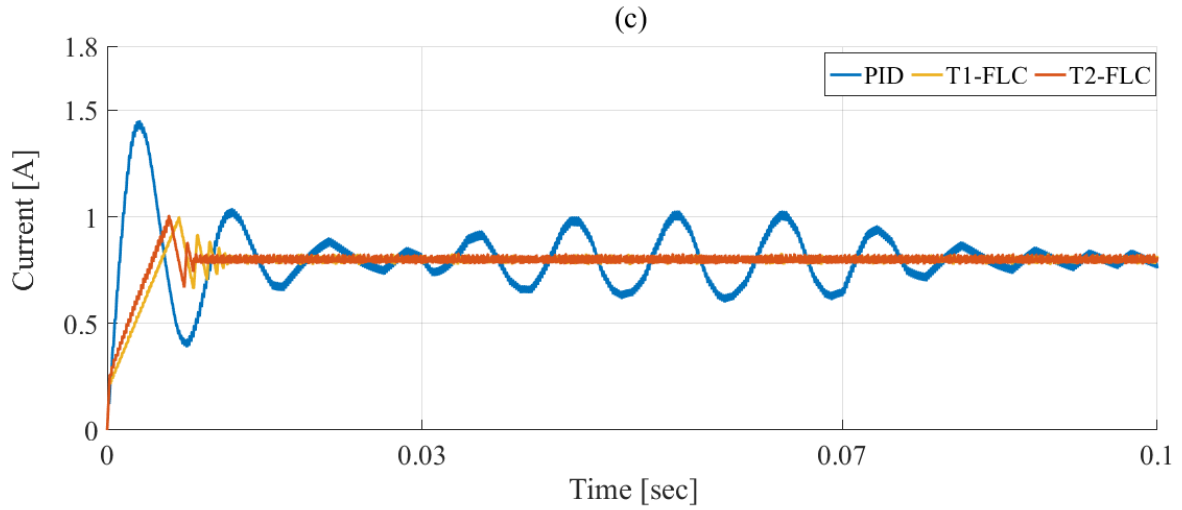

Figure II.16. Simulation results of the Buck converter with different controllers under dynamic input conditions: (a) output voltage, (b) inductor current.

Figures II.16 shows a comparison of the different controllers for this teste. It can be seen that the PI controller exhibits considerable deviations from the reference during these input fluctuations. This indicates its limited disturbance rejection capability under dynamic input conditions. In contrast, both the Type-1 and Type-2 fuzzy controllers demonstrate strong robustness, maintaining output stability with minimal deviation. The T2-FLC, in particular, effectively absorbs the impact of input disturbances, showing superior compensation and lower steady-state error compared to the other controllers.

These results confirm the enhanced adaptability and resilience of fuzzy logic controllers especially Type-2 in environments with unpredictable or fluctuating supply conditions.

II.5. Conclusion

In this chapter, we introduced the concept of fuzzy logic as a powerful tool for managing uncertainty and controlling complex, nonlinear systems. The fundamental principles and terminology of fuzzy logic were presented, including fuzzy sets, membership functions, rule bases, and the inference mechanism. The objective was to explore how fuzzy logic can be effectively applied to control a buck converter, a widely used DC-DC power electronic converter.

We began by designing a T1-FLC with PI structure, detailing the controller's structure and input/output variables. Although T1-FLC provides improved performance over conventional PID control in many cases, it faces limitations when dealing with high levels of uncertainty or dynamic operating conditions. To overcome these limitations, we introduced and implemented an advanced fuzzy logic paradigm type-2 fuzzy logic. A brief theoretical background of type-2

fuzzy sets and their structural components was presented. We then proceeded with the synthesis and simulation of T2-FLC with PI structure, highlighting its capability to manage uncertainty more effectively than its type-1 counterpart.

A comprehensive comparative study was conducted between the conventional PID controller, T1-FLC, and T2-FLC under several scenarios: nominal operating conditions, load resistance variations, output voltage tracking with various reference profiles, and input voltage disturbances. The results demonstrated that while all three controllers maintain basic regulation, the T2-FLC consistently outperforms both the PID and T1-FLC in terms of transient response, tracking accuracy, and robustness to disturbances.

In the next chapter, we will move from simulation to practice by presenting the real-time implementation of the intelligent-robust fuzzy controllers and assessing their performance in a practical environment.

Chapter III:

Real-time Implementation of Synthesized Controllers

III.1. Introduction

The transition from simulation to real-time implementation marks a critical phase in the validation of control strategies. While simulations provide a controlled environment to analyze system behavior and optimize parameters, they inherently rely on idealized assumptions and neglect various real-world complexities such as sensor noise, quantization effects, sampling delays, computational limitations, and unmodeled dynamics.

As Einstein wittily noted, "*In theory, everything works, but nothing functions; in practice, everything functions, but no one knows why*." This statement resonates profoundly in control engineering, where theoretical models often diverge from practical outcomes. Real-time implementation serves as the essential bridge between these two domains, enabling a realistic evaluation of the controller's robustness, reliability, and adaptability.

In this chapter, we present the real-time implementation of the controllers previously studied namely, the PID controller, T1-FLC, and type-2 FLC applied to a Buck converter. This phase involves addressing hardware integration, real-time constraints, and experimental validation. Through this process, we aim not only to test the effectiveness of each control strategy but also to refine our models and assumptions in light of practical observations.

III.2. Description of the experimental test bench

The experimental test bench was developed at the Electronics Department of the Farhat Abbas University of Sétif (Power Electronics and Industrial Control Laboratory (LEPCI)). As shown in Figure III.1, the test bench consists of a power circuit configured as a Buck converter, supplied by dedicated power supplies, sensing elements, and data acquisition components. The setup integrates a Semikron IGBT driver module, a voltage amplifier card (5-15V), ADC/DAC

interfaces, and a dSPACE 1104 control module. The entire system is supervised and monitored via a host PC equipped with MATLAB®/Simulink® and ControlDesk® software. The following sections provide a detailed description of each component of the test bench.

(a)

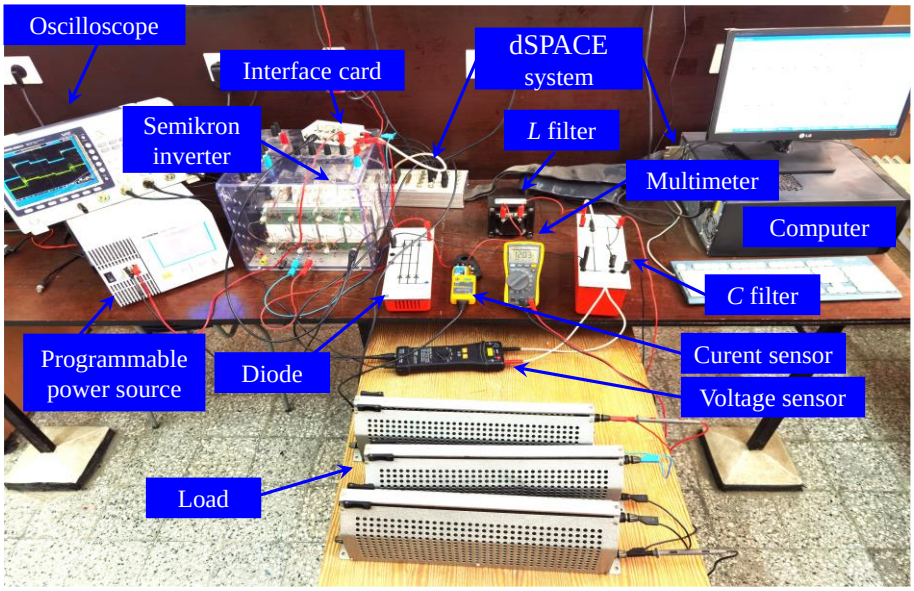

(b)

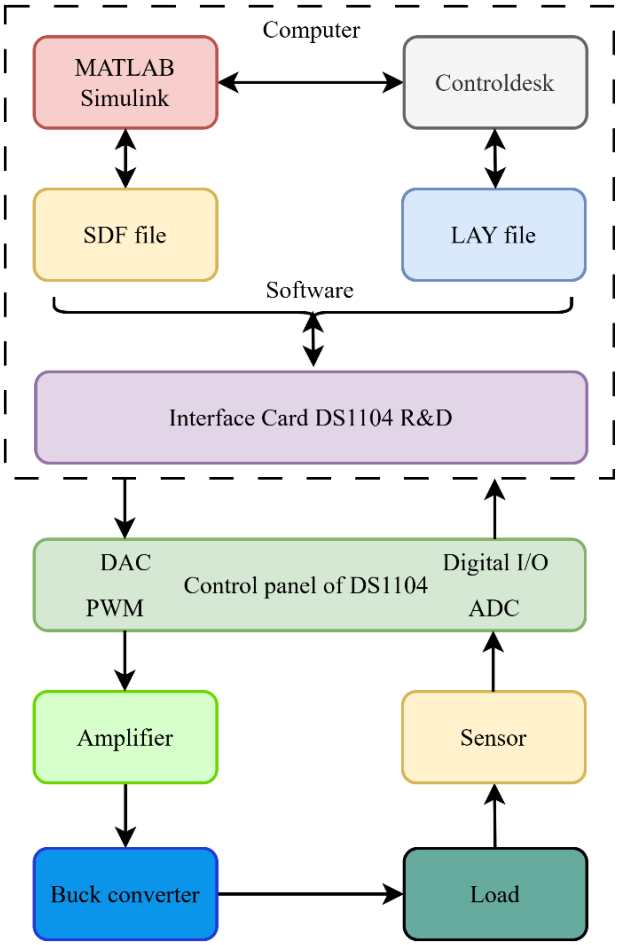

Figure III.1. (a) Photograph of the experimental test bench, (b) General schematic diagram of the test bench.

III.2.1. Power Supply Elements

The power supply elements are responsible for delivering stable and isolated energy to the various components of the test bench, ensuring safe and reliable operation of the Buck converter and its control circuit.

- *Main DC Power Supply*: A *GW Instek APS-1102A* programmable AC/DC power source Figure III.2(a) designed for precision testing of electronic equipment. It provides a wide range of output voltage and frequency settings, supporting both sinusoidal and arbitrary waveform generation; with a maximum output of 250 V AC and 1 kVA, this unit enables engineers to evaluate power converters, and other devices under controlled and repeatable AC or DC supply scenarios. The large front-panel display offers real-time readouts of voltage, current, power, and other electrical parameters, while the interface allows fine control over output mode, phase, and protection settings. This makes the *Instek APS-1102A* particularly suitable for the pre-compliance testing, inverter evaluation, and power electronics development.
- *Auxiliary Power Supplies*: A *GW Instek SPS-1820* DC power supply Figure III.2(b) used in lab environments to provide a stable and adjustable DC voltage (0–15 V) and current (up to 3 A). It features dual digital displays for voltage and current, with fine and coarse adjustment knobs for precise control. The supply operates in constant voltage or constant current mode depending on the load, and includes safety features such as current limiting. Its reliability and precision make it suitable for real-time control validation.

(a) (b)

Figure III.2. (a) Programmable power supply and (b) DC power supply.

III.2.2. Buck Converter Elements

In the Buck converter configuration, the Semikron IGBT module (Figure III.3(a)) serves as the main power switch, driven by gate signals from the dSPACE control platform. The power

stage also includes a diode (Figure III.3(b)), an inductor of 30mH (Figure III.3(c)), and a capacitor of 500µF (two 1000µF capacitors connected in series, Figure III.3(d)) arranged to emulate a realistic Buck converter topology. The inductor is placed in series with the output to regulate current rise time, while the capacitor is connected in parallel with the load to smooth the output voltage and reduce ripple and the diode and the diode is connected in antiparallel with the switch to provide the current path during off periods. The load stage is composed of three resistive elements of 5Ω each, connected in series, forming a 15Ω total resistive load.

This arrangement replicates practical load conditions and switching dynamics, providing an accurate representation of converter behavior under real-time operation.

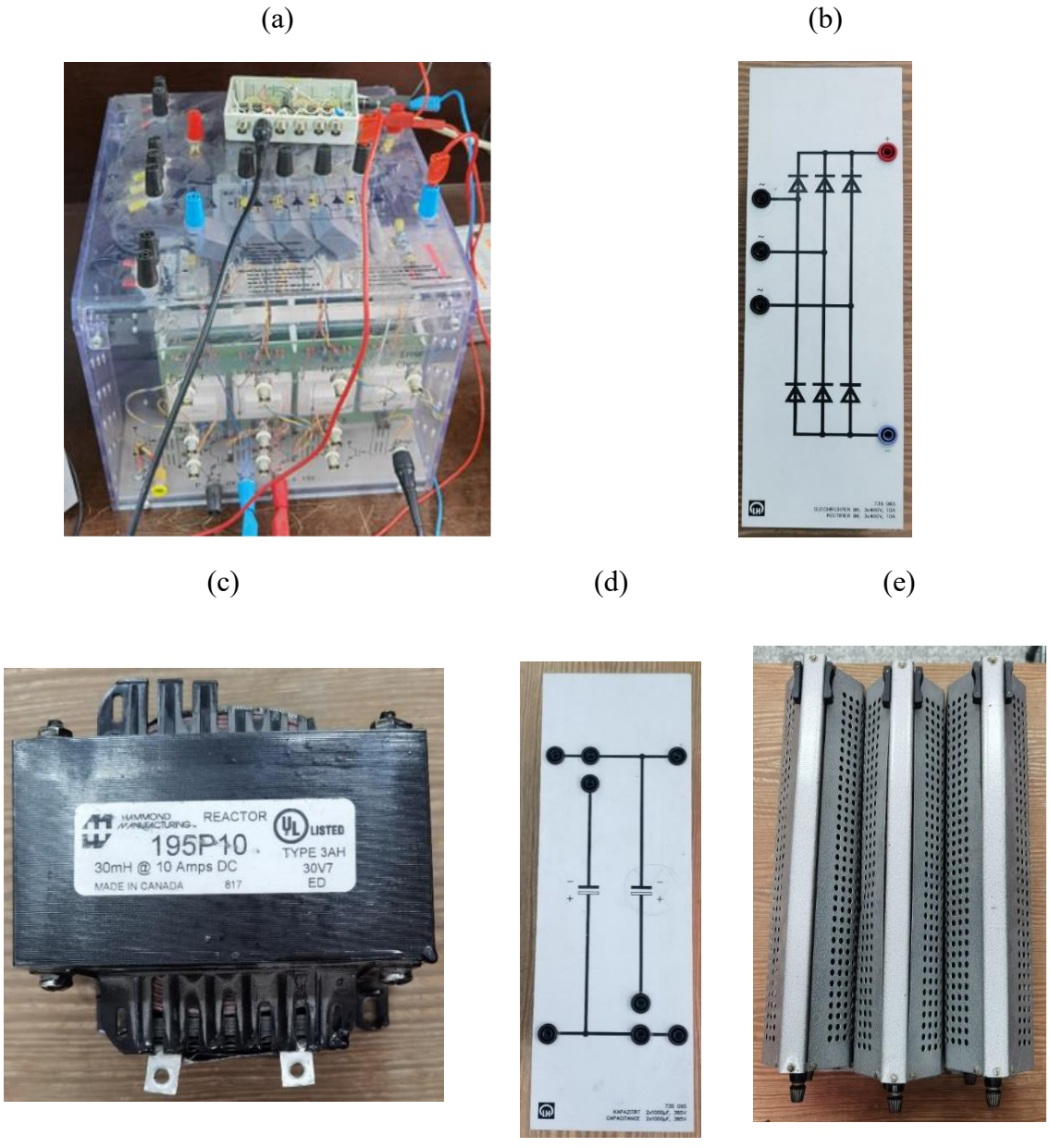

Figure III.3. (a) Semikron module, (b) Diode, (c) 30mH inductor, (d) Capacitor bank (two 1000µF capacitors), and (e) Resistive load (three 5 Ω resistors).

III.2.3. Sensing and Measurement Elements

Sensing and measurement elements are essential for acquiring accurate real-time data on voltage and current within the Buck converter system. These elements ensure reliable monitoring and validation of control performance during experimental implementation.

- *Voltage senso-GW Instek GDP-050*: The *GW Instek GDP-050* (Figure III.4(a)) is a high-voltage differential probe designed for safe and accurate voltage measurements between two points in a floating circuit. With a bandwidth of 50 MHz, it converts high-voltage floating signals into low-voltage ground-referenced signals suitable for display on any standard oscilloscope via a BNC connector. The *GDP-050* supports multiple selectable attenuation settings (×100, ×200, ×500, ×1000), offering flexibility for a wide range of applications. It also includes various probe tip accessories for different measurement scenarios and features an over-range indicator to warn users when input signals exceed the probe's dynamic range.

- *Current sensor-Fluke i310s AC/DC current clamp probe:* The *Fluke i310s* (Figure III.4(b)) is a precision instrument used for non-intrusive current measurements. This clamp operates using a combination of Hall effect sensing for DC currents and transformer-based sensing for AC signals, enabling accurate measurement of currents up to 100 A. It provides a voltage output proportional to the measured current, typically at 100 mV/A or 10 mV/A depending on the selected sensitivity range. The probe connects directly to an oscilloscope or data acquisition system via a standard BNC connector, allowing for real-time monitoring of current waveforms. Its clamp-on design permits measurements without the need to disconnect or interrupt the circuit, enhancing safety and measurement convenience. This makes it particularly effective for analyzing current during real-time experimental validation.

- *Multimeter-FLUKE Digital True RMS*: The *FLUKE Digital True RMS* (Figure III.4(c)) is a precision instrument designed for accurate electrical measurements in both AC and DC circuits. Unlike average-responding meters, this True RMS meter provides correct readings for non-sinusoidal waveforms; it can measure voltage, current, resistance, continuity, frequency, and temperature with high accuracy and stability. Its robust build, overload protection, and backlit display make it suitable for both laboratory and field use. In a control implementation setup, it is essential for validating sensor outputs, verifying power supply levels, and ensuring safe operation during real-time testing.

- *Oscilloscope-GW Instek GDS-3504:* The *GW Instek GDS-3504* (Figure III.4(d)) is a 500 MHz, 4-channel digital storage oscilloscope designed for advanced signal analysis in high-speed electronic systems. With a sampling rate of up to 5 GSa/s and deep memory depth, it allows precise capture and visualization of transient events. This model supports advanced triggering, automatic measurements, FFT analysis, and multi-window display, offering engineers comprehensive insight into voltage and timing behaviors. Its high-resolution display and intuitive interface make waveform analysis efficient and reliable during real-time testing and controller validation.

(a) (b)

(c) (d)

Figure III.4. (a) Voltage sensor, (b) Current sensor, c) Multimeter and (d) Oscilloscope.

III.2.4. Control Unit Elements

The control unit is at the heart of the experimental setup, responsible for implementing, executing, and supervising the control strategies applied to the Buck converter in real time. It is primarily composed of the dSPACE DS1104 real-time control platform and the ControlDesk® software environment.

- *dSPACE DS1104 Real-Time Control Platform*: The *DS1104* is real-time control platform is a powerful development system used in academia and industry for rapid prototyping of real-time control algorithms. It integrates both signal acquisition and

real-time computation in one unit, enabling seamless implementation and validation of PID, type-1, and type-2 fuzzy logic controllers. The DS1104 system consists of two primary components [10]:

1. *Processor Board (DSP Interface Card)*: Installed in a host computer via the PCI slot, this board is equipped with a high-performance floating-point DSP. It handles real-time execution of control algorithms, enabling high-speed data processing and deterministic control. The DSP board interfaces directly with MATLAB/Simulink via the Real-Time Interface , allowing for automatic code generation and compilation of control models.
2. *I/O Panel (Front Panel* (Figure III.5)*)*: This front-end hardware features:
   - 8 analog input channels (ADC) via BNC connectors;
   - 8 analog output channels (DAC) via BNC connectors;
   - PWM channels for driving switching devices such as IGBTs in converters.
   - Incremental encoder inputs, digital I/O, and serial communication ports (RS232, RS422) to support various peripheral interfaces.

To interface the *DS1104* with the SEMIKRON power module, a custom interface card was used to adapt the control signals. This card adapts the control signals to meet the voltage and current requirements of the driver stage.

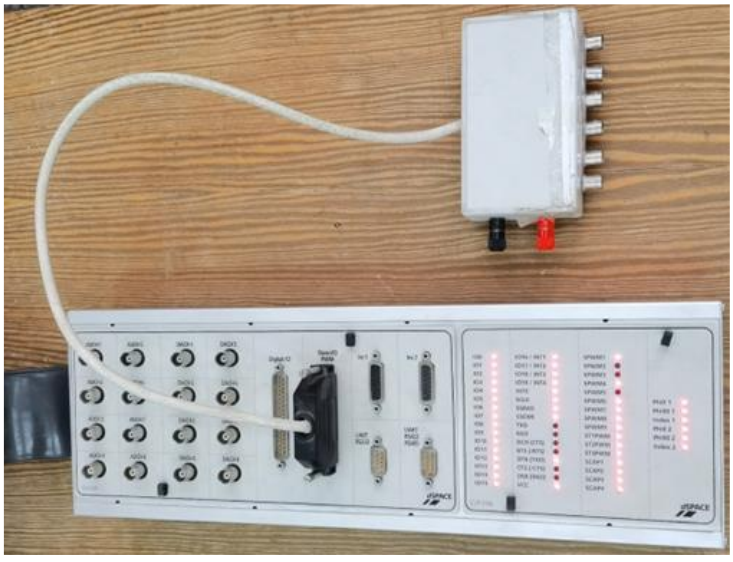

Figure III.5. I/O Panel of the dSPACE DS1104 system.

- *ControlDesk® Software*: *ControlDesk®* is a graphical user interface software developed by dSPACE for monitoring and interacting with real-time control systems. In this setup, it serves as a supervisory tool, offering:

- Real-time parameter tuning;
- Visualization of signals (voltages, currents, control outputs, etc.);
- Data logging for offline analysis;
- Manual override and setpoint adjustment

III.3. Experimental Result

This section presents the experimental validation of the implemented control strategies under real-time conditions. Following the detailed description of the test bench, we evaluate the performance of the PI, type-1 FLC, and type-2 FLC controllers applied to a DC-DC Buck converter. The fuzzy logic controllers were implemented in Simulink® using a lookup table-based approach. Instead of using on the standard Fuzzy Logic Controller block, we generated rule surfaces programmatically using MATLAB® scripts. These surfaces were then exported as precomputed 2D matrices, forming the basis of 2D Lookup Table blocks. The controller inputs error e and change in error de are mapped to the lookup table indices (See appendix). This method eliminates the need for real-time fuzzy inference, reducing computational load while maintaining the behavior of the fuzzy rule base and membership functions.

The performance of each controller is assessed under various operating scenarios, including nominal conditions, load resistance changes, reference voltage tracking, and input voltage disturbances. This experimental setup allows us to analyze the controllers' dynamic response, steady-state accuracy, and robustness to external perturbations, confirming their effectiveness beyond simulation environments.

All controllers are implemented with a sampling time of 0.1 ms, and the switching frequency of the Buck converter is set to 10 kHz

III.3.1. Performance Evaluation under Output Voltage Reference Tracking

To begin the experimental evaluation, Figures III.6 and III.7 illustrates the real-time step response of the Buck converter with different controllers in response to sudden changes in the output voltage reference. While all controllers demonstrated satisfactory steady-state tracking, notable differences were observed during the transient phase. The PID controller exhibited larger overshoot and longer settling time compared to its fuzzy counterparts. Both the type-1 and type-2 fuzzy controllers provided smoother and faster responses, with the T2-FLC showing a marginally superior dynamic performance evidenced by reduced overshoot and quicker stabilization. These results confirm the practical advantage of fuzzy control, particularly the enhanced adaptability of the T2-FLC in handling abrupt reference changes. Table III.1

summarizes the experimental performance of the Buck converter under a step reference change from 0 V to 12 V using three control strategies.

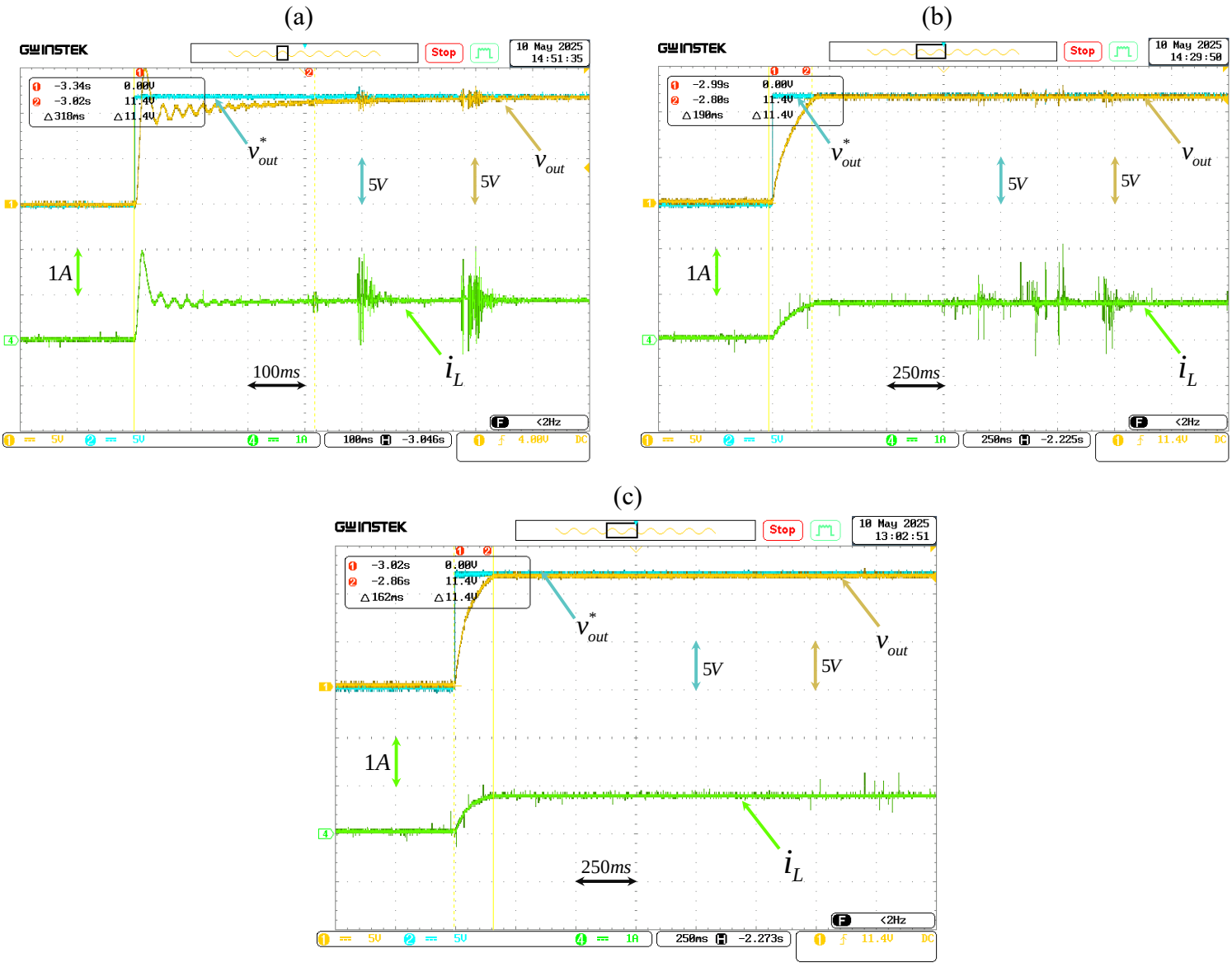

Figure III.6. Experimental results of the output voltage and inductor current of the Buck converter with different controllers under a step change in the output reference voltage from 0 V to 12 V: (a) PID Controller, (b) T1-FLC, and (c) T2-FLC.

Table III.1. Experimental key performance metrics of the Buck converter using different controllers under a step change in the output reference voltage from 0 V to 12 V.

Controller	Settling time [sec]	Overshoot [V]
PID	0.32	4.98
T1-FLC	0.19	0.1
T2-FLC	0.16	0

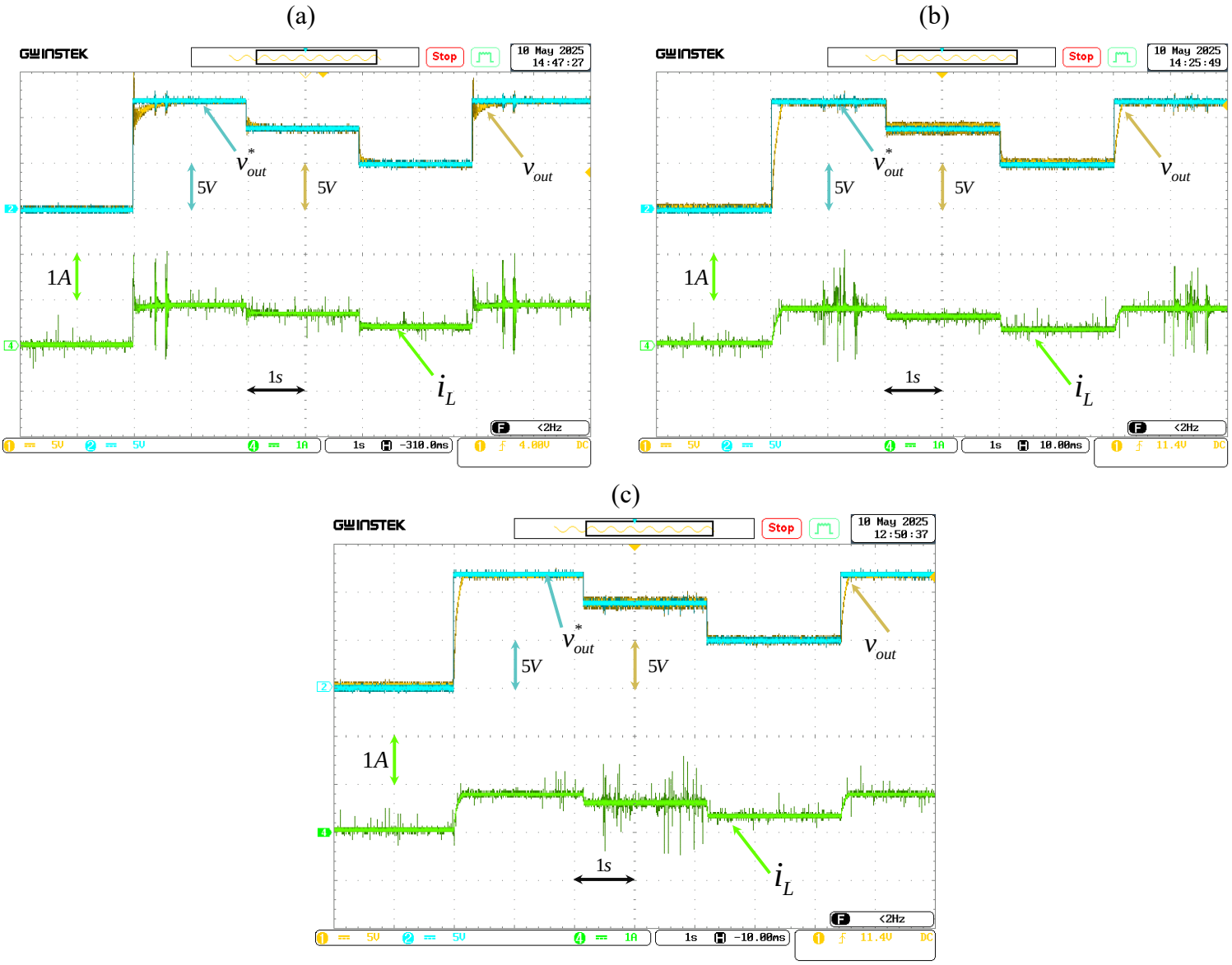

Figure III.7. Experimental results of the output voltage and inductor current of the Buck converter with different controllers under step changes in the output reference voltage: (a) PID Controller, (b) T1-FLC, and (c) T2-FLC.

To further evaluate dynamic tracking capabilities, the Buck converter was tested under sinusoidal and triangular reference voltage profiles. These waveforms were chosen to emulate smooth and continuously varying setpoints, challenging the controllers' ability to maintain accurate and responsive output regulation.

As shown in Figures III.8 and III.9, the PID controller struggled to follow the time-varying reference signals, exhibiting noticeable lag and tracking error. The T1-FLC demonstrated improved responsiveness and reduced steady-state error under both test profiles. However, the T2-FLC consistently outperformed both alternatives, offering faster transient response and more precise tracking with minimal overshoot or delay. These experimental results reinforce

the advantages of type-2 fuzzy control in applications requiring accurate real-time adaptation to smoothly varying setpoints.

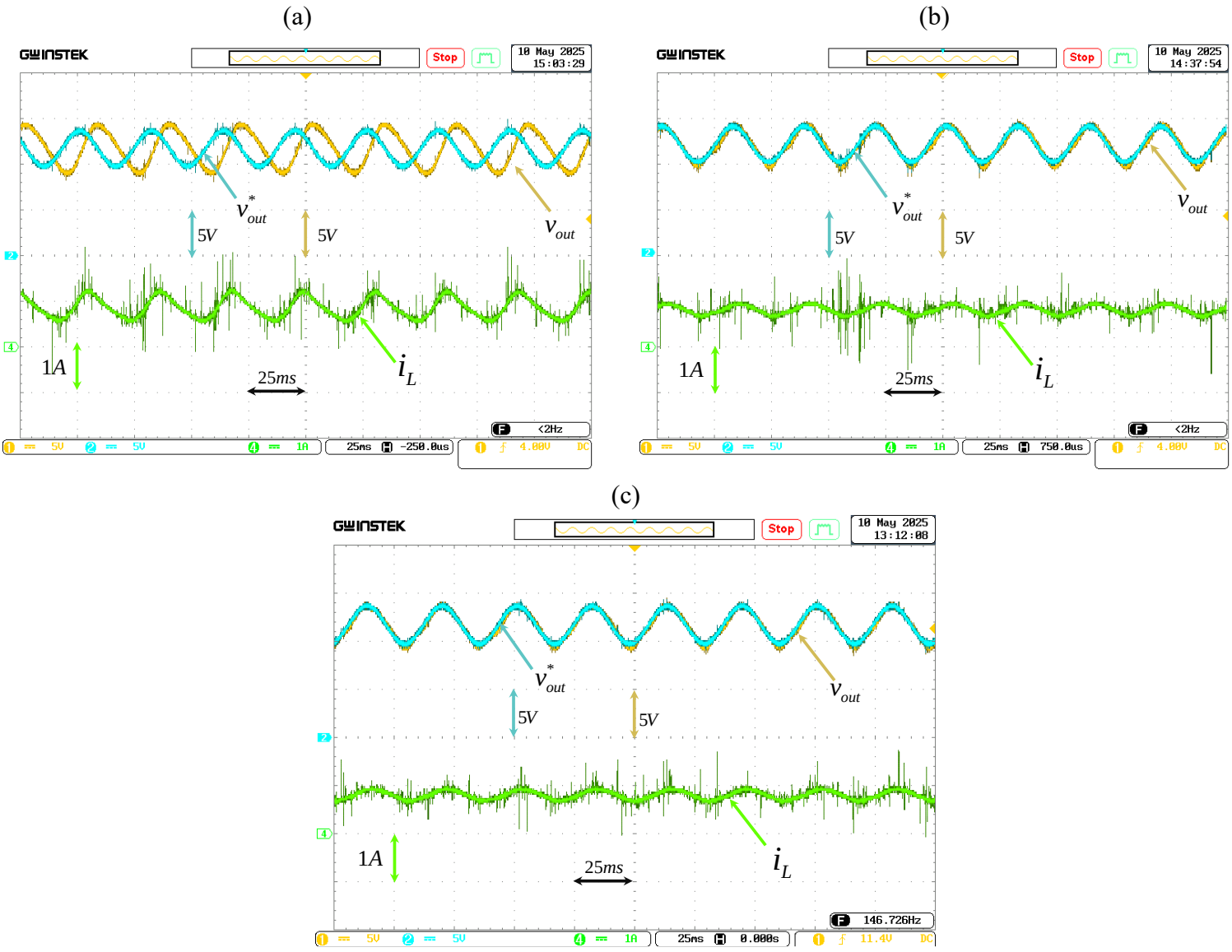

Figure III.8. Experimental results of the output voltage and inductor current of the Buck converter with different controllers under sinusoidal-wave tracking: (a) PID Controller, (b) T1-FLC, and (c) T2-FLC.

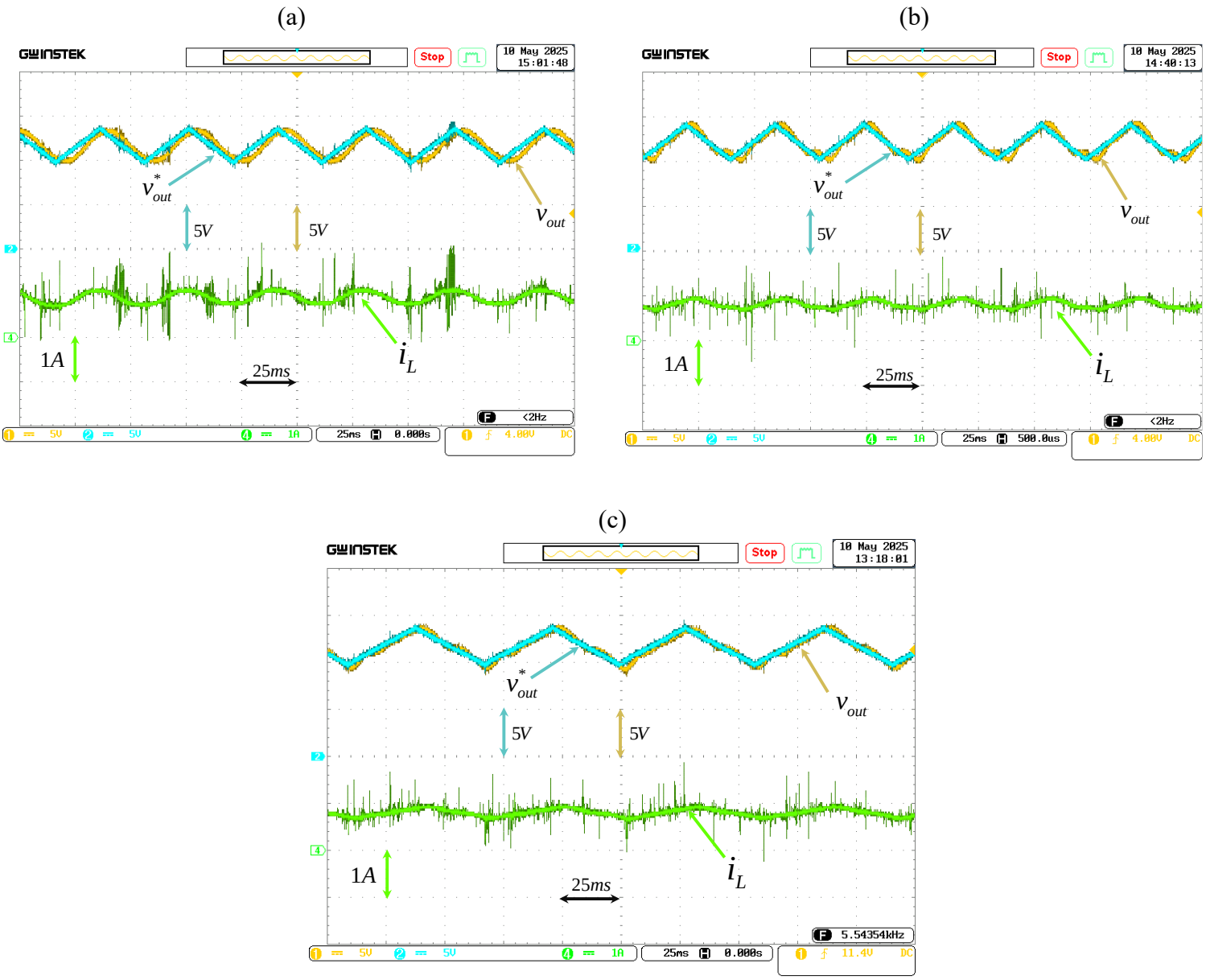

Figure III.9. Experimental results of the output voltage and inductor current of the Buck converter with different controllers under triangular-wave tracking: (a) PID Controller, (b) T1-FLC, and (c) T2-FLC.

III.3.2. Performance Evaluation under Load Variations

In this experiment, the performance of the three controllers was assessed under sudden load disturbances a step change in resistive load from 15 Ω to 7.5 Ω and back to 15 Ω while keeping the output voltage reference fixed at 12 V. The results, shown in Figure III.10, highlight how each controller responded in real time to these abrupt variations. All three controllers eventually restored the output voltage, but the transient behavior differed significantly. The PID controller exhibited noticeable voltage deviations and slower recovery, while the T1-FLC improved both

settling time and stability. The type-2 FLC delivered the best performance, responding more quickly with minimal overshoot and undershoot. These practical results demonstrate the 2-FLC's enhanced robustness and its superior ability to reject load disturbances effectively.

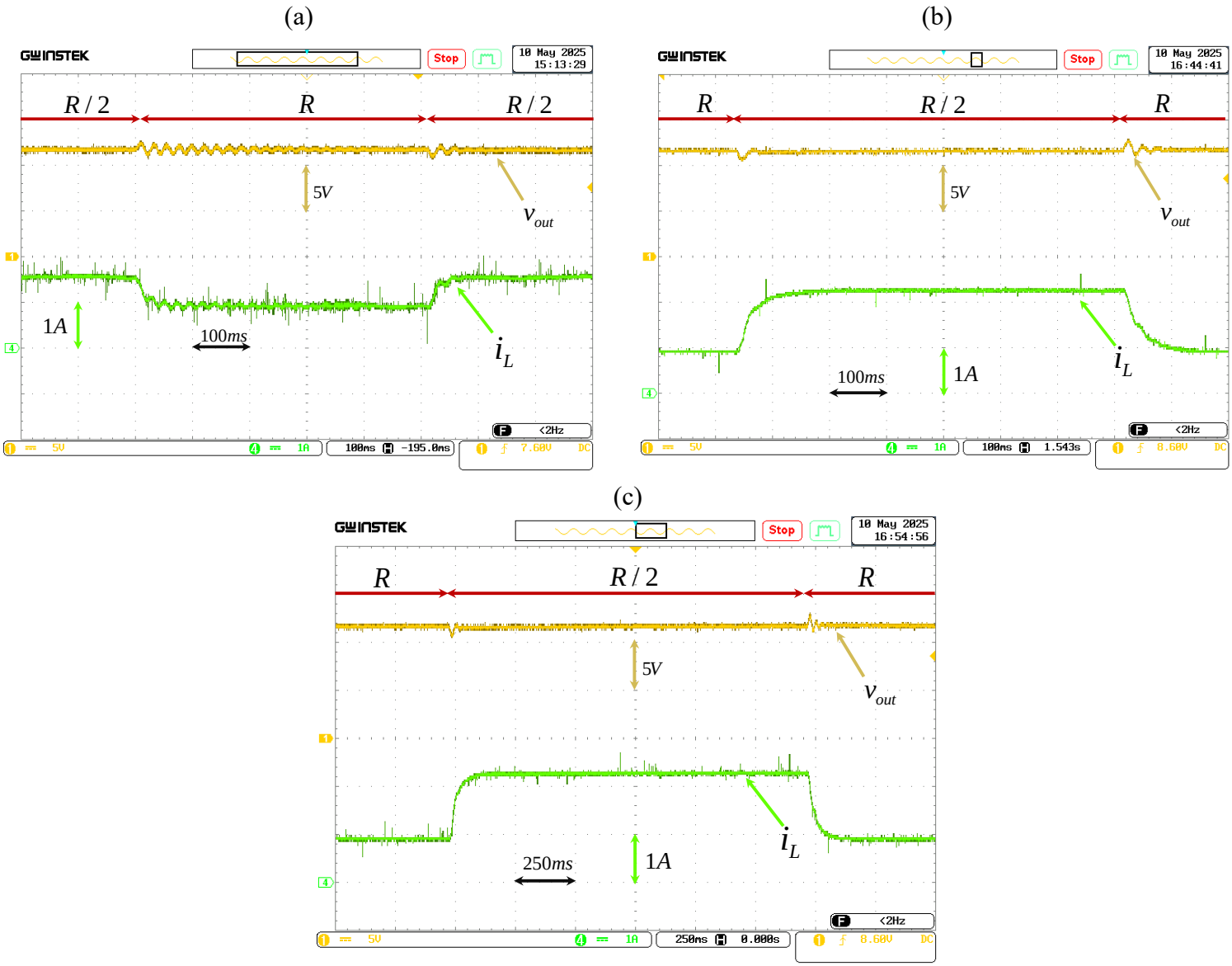

Figure III.10. Experimental results of the output voltage and inductor current of the Buck converter with different controllers under step changes in the resistive load: (a) PID Controller, (b) T1-FLC, and (c) T2-FLC.

III.3.3. Performance Evaluation under Input Voltage Disturbances

In this experimental setup, the Buck converter was subjected to varying input voltage conditions to assess the resilience of each control strategy. A composite voltage waveform was applied to the input to simulate realistic and dynamic disturbances. Throughout the test, the output voltage was regulated to a constant 12 V.

As shown in Figure III.11, the PID controller struggled under these non-ideal conditions, displaying significant deviations from the reference voltage. This highlights its limited ability

to reject input-side disturbances. In contrast, both fuzzy controllers-maintained output regulation more effectively. The T1-FLC handled the fluctuations with improved stability, while the T2-FLC exhibited the most robust behavior, delivering minimal deviation and quicker recovery throughout the test. These real-time results confirm the superior disturbance rejection and adaptability of the T2-FLC, making it particularly suitable for applications exposed to unpredictable supply variations.

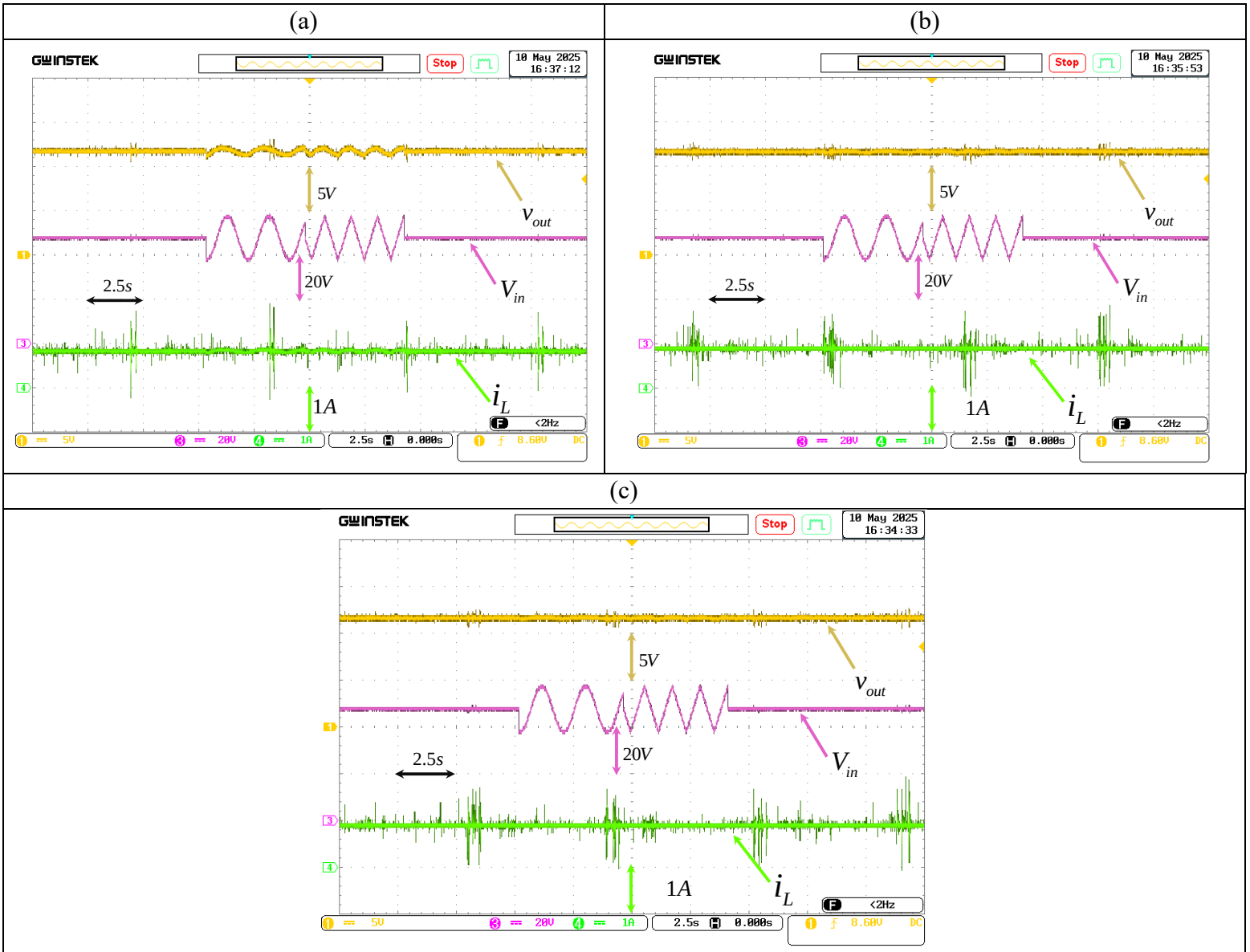

Figure III.11. Experimental results of the output voltage and inductor current of the Buck converter with different controllers under dynamic input conditions: (a) PID Controller, (b) T1-FLC, and (c) T2-FLC.

III.4. Conclusion

This chapter has demonstrated the practical deployment of the PID, type-1 and type-2 fuzzy logic controllers in real-time operation for regulating a DC-DC Buck converter. By integrating

these control strategies into an experimental test bench and observing system behavior using precision instrumentation (oscilloscope, multimeter, and dSPACE interface), we validated their performance under real-world conditions beyond what simulation alone could provide.

The PID controller, while straightforward to implement, showed clear limitations in managing nonlinear dynamics and parameter shifts. The type-1 fuzzy logic controller offered improved transient response and better adaptation to changing conditions. However, the type-2 fuzzy logic controller distinguished itself by delivering the most robust and accurate performance thanks to its ability to model uncertainty. It consistently minimized overshoot, reduced steady-state error, and handled disturbances more effectively than the other two approaches.

In summary, real-time results confirmed the theoretical advantages of fuzzy logic particularly type-2 controller as a high-performance control solution for power electronics applications. This highlights their potential as a reliable and adaptable alternative for demanding and uncertain operating environments.

General Conclusion

This thesis presented a detailed investigation on the modeling, design, simulation, and real-time implementation of control strategies for a DC-DC Buck converter. The focus was placed on evaluating and comparing conventional proportional-integral-derivative (PID) control with intelligent fuzzy logic-based approaches, type-1 and type-2 fuzzy logic controllers (FLCs), in terms of system stability, robustness against parameter variations and disturbances, and dynamic performance.

Chapter 1 established the theoretical groundwork by investigating the fundamentals of DC-DC converters, with particular emphasis on the Buck converter. It also includes the design, analysis, and simulation of a classical PID controller using MATLAB®/Simulink®. In chapter 2, the study progressed into intelligent control strategies. The structures and operating mechanisms of type-1 and type-2 FLCs were explored in detail, highlighting the key functional blocks: fuzzification, inference, rule base, defuzzification, and type-reduction (for type-2 FLC). A comprehensive comparative simulation study was conducted using MATLAB®/ Simulink®, assessing the performance of the PID controller, type-1 FLC, and type-2 FLC under various operating conditions. These include nominal operation, load resistance variations, output voltage tracking under different reference profiles, and input voltage disturbances. Chapter 3 transitioned to real-time implementation using the dSPACE DS1104 platform and ControlDesk software. The PID, type-1 FLC, and type-2 FLC controllers were implemented and tested under practical scenarios similar to those examined in simulation.

In conclusion, the type-2 FLC outperformed both the PID and type-1 FLC controllers by exhibiting enhanced dynamic performance, greater adaptability, and superior robustness against perturbations and external disturbances, as validated through both simulation and experimental results. Therefore, the type-2 FLC presents a promising solution for advanced power electronic applications that demand high precision, reliability, and resilience in the presence of uncertainties and varying operating conditions.

Future studies may focus on the integration of adaptive or self-tuning fuzzy systems, the exploration of hybrid control strategies, and the application of multi-objective optimization techniques to further enhance performance across a wider range of operating conditions.

Appendix

- ***Performance Evaluation Indices:***

To quantitatively assess the dynamic behavior and regulation quality of the implemented controllers (PID, Type-1 FLC, and Type-2 FLC), the following standard performance indices were used. Each index captures different aspects of control performance, particularly during transient response under step or disturbance conditions:

Parameter	Equations	Note
Integral of Absolute Error	$IAE = \int_0^T \lvert e(t) \rvert dt$	Used to measure the total accumulated error over time. In this work, IAE was used to evaluate the general tracking accuracy of each controller. A lower IAE indicates better error minimization.
Integral of Squared Error	$ISE = \int_0^T e^2(t)dt$	Emphasizes larger errors more strongly. This index was helpful in comparing how each controller handles large deviations during transients. Lower ISE suggests better suppression of large error magnitudes.
Integral of Time-weighted Absolute Error	$ITAE = \int_0^T t \,.\, \lvert e(t) \rvert dt$	Penalizes late-occurring errors more than early ones. In this study, ITAE was used to highlight the controller's settling behavior and responsiveness over time. Lower ITAE means the system stabilizes faster with minimal lingering error.
Integral of Time-weighted Squared Error	$ITSE = \int_0^T t \,.\, e^2(t)dt$	Combines time sensitivity and squared error weighting. Applied here to evaluate both the amplitude and duration of transient errors. Lower ITSE reflects quicker damping of large errors and better dynamic response.

- ***Description of the Real-Time Simulink Model Architecture***

The following Simulink diagram corresponds to the real-time implementation of the control strategies developed for the DC-DC buck converter using the dSPACE DS1104 platform. The signal processing chain begins with analog signal acquisition via DS1104ADC channels, followed by low-pass filtering blocks to suppress high-frequency noise and ensure cleaner signal inputs.

Gain blocks are strategically included to compensate for attenuation introduced by sensors and ADC scaling. A fixed gain of 1.5 is used to offset the inherent sensor bias and center the voltage measurement around zero for accurate feedback control.

Within the control loop, fuzzy logic controllers are implemented with error signals normalized through adjustable gains (e.g., k_e, k_{de}) to align with the normalized fuzzy membership domains. The reference voltage (Vref) is used to generate the control error, which is then processed by the fuzzy inference engine to compute the required control action.

The resulting control output (duty cycle α) is sent to the PWM generation block (DS1104SL_DSP_PWM3) to drive the converter. Simultaneously, selected internal signals are routed through DAC channels for real-time observation and analysis. Final output signals are rescaled via denormalization gains (e.g., 1/100, 1/10) to match physical actuator voltage levels.

This implementation structure ensures accurate closed-loop control while maintaining real-time compatibility and observability.

(a)

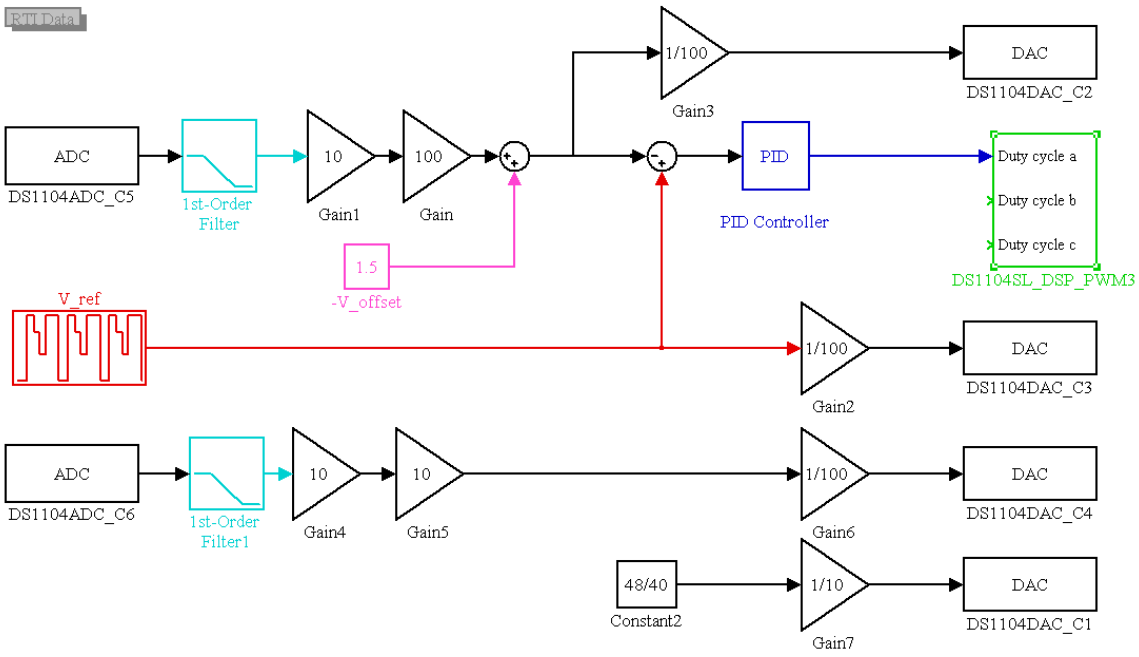

(b)

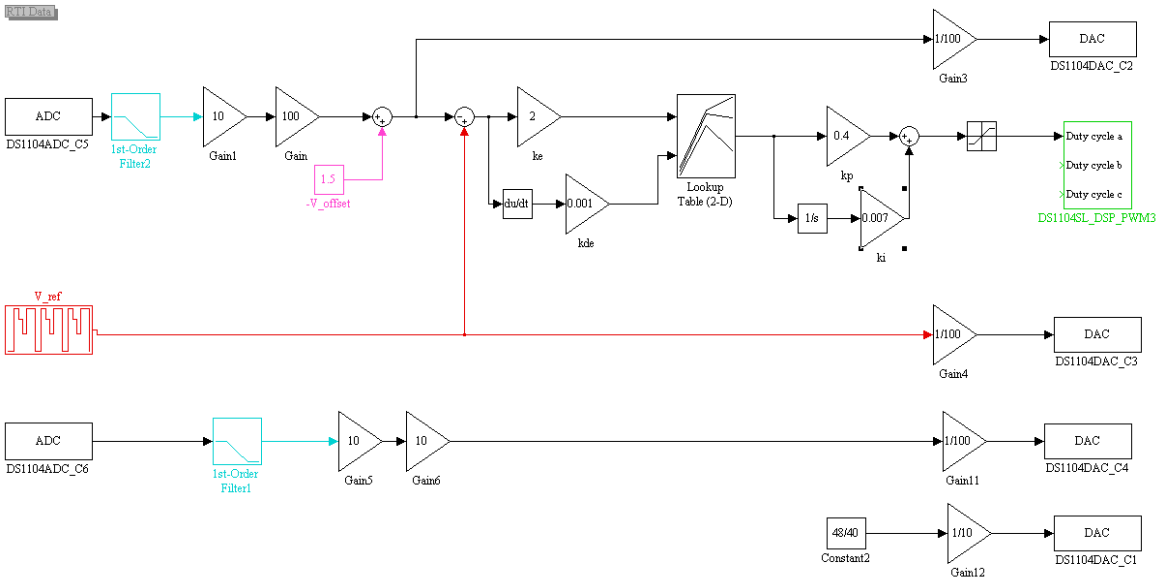

(c)

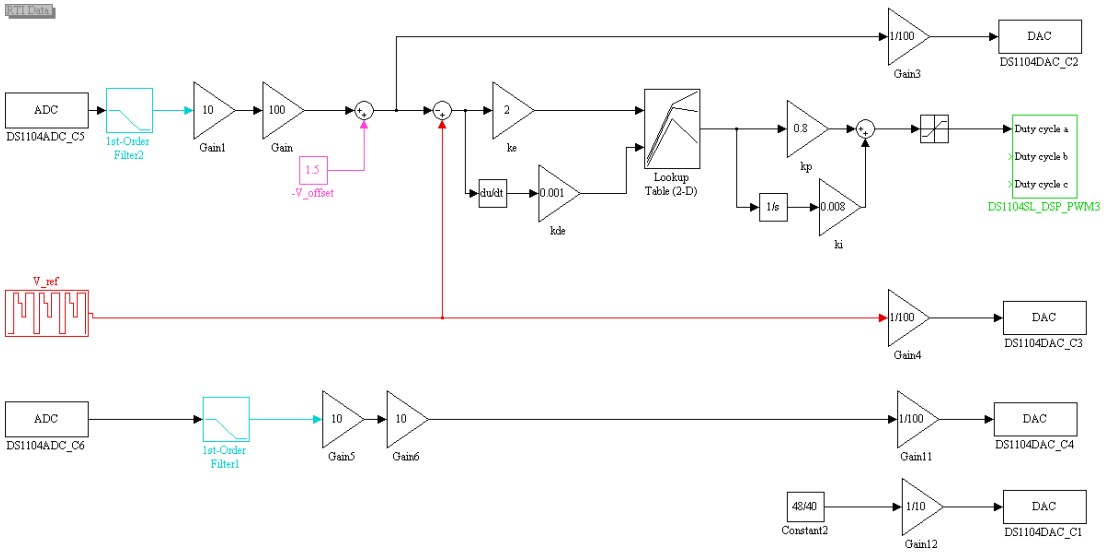

Figure A.1.(a). Simulink diagram of PID controller, (b) Simulink diagram of T1-FLC controller, (c) Simulink diagram of T2-FLC controller.

Bibliography

[1] Ned Mohan , Tore M. Undeland , William P. Robbins, Power electronics, New york , Toronto , Singapore: JOHN WILEY & SONS, INC., 1995.

[2] Muhammad H. Rashid , J. David Irwin, Power Electronics Handbook, SAN DIEGO , SAN FRANCISCO , NEW YORK , BOSTON , LONDON , SYDNEY , TOKYO: Auburn University , Acadimic press, 2001.

[3] Guanrong Chen ,Trung Tat Pham, Introduction to Fuzzy sets , Fuzzy Logic , and Fuzzy Control Systems, Florida: CRC Press, 2000.

[4] L.-X. Wang, A course on Fuzzy Logic systems and control, Hong Kong: The Hong Kong Universty of Science and Technology.

[5] Robert W. Erickson , Dragan Maksimovi´c, Fundamentals of Power Electronics, USA: Springer, 2001.

[6] M. H. Rashid, Power Electronics Handbook Devices, Circuits, AND Applications, Burlington: University of West Florida, 2011.

[7] K. Guesmi, Contribution à la commande floue d'un convertisseur statique, Université de Reims Champagne Ardenne, 2019.

[8] V. Vodovozov, Introduction to power electronics, Jerry M. Mendel and Robert I. Bob John, 2010.

[9] Chuen Chien Lee , Student member, IEEE, "fuzzy logic in control systems: Fuzzy Logic controller _ Part I," *IEEE Transactions On Systems, Man, and Cybernetics,* vol. 20, pp. 404-418, 1990.

[10] B. Abdelouahab, Techniques De Commande Predictive ET Floue, SETif: Universite Ferhat Abbas - Setif, 2010.

[11] Dr.T.Govindaraj, Rasila R, "Development of Fuzzy Logic Controller for DC – DC Buck Converters," *techsciencepub,* vol. II, pp. 192-198, 2011.

[12] S. Nabil, Implantation d'un contrôleur flou de ventilation d'un tunnel, Setif: Universite Ferhat Abbas - Setif, 2011.

[13] Z. Nadjat, Contribution au Contrôle Robuste des Convertisseurs DC-DC, Batna : Université de Batna 2 – Mostefa Ben Boulaïd, 2018.

[14] Rabah Araria, Abderrahmane Berkani, Karim Negadi, Fabrizio Marignetti, Mohamed Boudiaf, "Performance Analysis of DC-DC Converter and DTC Based Fuzzy Logic Control for Power Management in Electric Vehicle Application," *Journal Européen des Systèmes Automatisés,* vol. 53, 2020.

[15] George J. Klir , Bo Yuan, Fuzzy sets and Fuzzy Logic Theory and Applications, Binghamton, New York: Prentice Hall PTR, 1995.

[16] K. H. Lee, First Course on Fuzzy Theory and Applications, Berlin Heidelberg NewYork: Springer, 2005.

[17] D. Wu, "A Brief Tutorial on Interval Type-2 Fuzzy Sets and Systems," *researchgate,* pp. 1-14.

[18] Qilian Liang and Jerry M. Mendel, Fellow, IEEE, "Interval Type-2 Fuzzy Logic Systems:Theory and Design," *IEEE Transactions On Fuzzy Logic,* vol. 8, pp. 535-550, 2000.

[19] M. Manceur, Commande robuste des systèmes non, l'Université de Reims Champagne-Ardenne, 2012.

[20] M. Almaraashi , R. John , A. Hopgood , S. Ahmadi , "Learning of interval and general type-2 fuzzy logic systems using simulated annealing: Theory and practice," *Elsevier,* pp. 2-42, 2016.

[21] Sathish Kumar Kollimalla, Student Member, IEEE and Mahesh Kumar Mishra, Senior Member, IEEE, "A Novel Adaptive P&O MPPT Algorithm Considering Sudden Changes in the Irradiance," *IEEE,* pp. 1-9, 2014.

[22] D. W. W. W. Tan, "A simplified type-2 fuzzy logic controller for real-time control," *ISA Transactions,* vol. 45, pp. 503-516, 2005.

[23] F. Paul Nishanth , Saroj Kumar Dash , Soumya Ranjan Mahapatro , "Critical study of type-2 fuzzy logic control from theory to applications: A state-of-the-art comprehensive survey," *elsevier,* vol. 10, 2024.

[24] Nikhil D. Bhat ,Swapnil D. Patil, Digvijay B. Kanse, Suraj D. Pawar, "DC/DC Buck Converter Using Fuzzy Logic Controller," *IEEE Xplore,* 2020.

[25] Dongrui Wu, Member, IEEE, "A Constrained Representation Theorem for Interval Type-2 Fuzzy Sets UsingConvex and Normal Embedded Type-1 Fuzzy Sets,and Its Application to Centroid Computation," *Global Research.*

[26] Shaik Gousia begum, Syed Sarfaraz Nawaz, "A study of Comparative analysis of fuzzy logic controller and neural network for dc–dc buck converter," *EDP Sciences,* 2021.

[27] H.-J. Zimmermann, Fuzzy Set Theory-and Its Applications, 4th ed., New York: Springer Seience+Business Media, 2001.

[28] Ummaleti SaiSangeeth, N. K. Arun, "Fuzzy Logic Control of DC-DC Buck Converter in DC Distribution System with Constant Power Load," pp. 180-191, 2023.

[29] T. J. Ross, Fuzzy Logic With Engineering Applications, 2nd ed., New Mexico, USA: University of New Mexico, USA, 2004.

[30] Juan R. Castro, Oscar Castillo, Luis G. Martínez, "Interval Type-2 Fuzzy Logic Toolbox," *Engineering Letters,* 2007.

[31] Jerry M. Mendel, Life Fellow, IEEE, Robert I. John, Member, IEEE, and Feilong Liu, Student Member, IEEE, "Interval Type-2 Fuzzy Logic Systems Made Simple," *IEEE Transactions on Fuzzy Systems,* vol. 14, pp. 808-821, 2006.

[32] F. Martin McNeill,Ellen Thro, Fuzzy Logic A Practical Approach, Boston, San Diego, New York, London, Sydney, Tokyo, Toronto: AP Professional, 1994.

[33] A. T. Azar, "Overview of Type-2 Fuzzy Logic Systems," *International Journal of Fuzzy System Applications,* pp. 1-28, 2012.

[34] Nilesh N. Karnik, Jerry M. Mendel, Fellow, IEEE, and Qilian Liang, "Type-2 Fuzzy Logic Systems," *IEEE Transactions On Systems,* vol. 7, pp. 643-658, 1999.

[35] Jerry M. Mendel , Robert I. Bob John, "Type-2 Fuzzy Sets Made Simple," *IEEE Transactions On Fuzzy Systems,* vol. 10, pp. 117-127, 2002.

[36] Prof. S. Samanta, Antip Ghosh, Mayank Kandpal, State-space average Modeling of DC-DC Converters with parasitic in Discontinuous Conduction Mode (DCM)., Rourkela: Department of Electrical Engineering National Institute of Technology, 2010.

[37] Abraham I. Pressman, Keith Billings, Taylor Morey, Switching Power Supply Design, USA: Mc Graw Hill, 2009.

[38] N. P. Keong, Small Signal Modeling Of DC-DC Power Converters Based ON Separation OF Variables, National University OF Singapore, 2003.

R. L. Gour, "Small Signal Modelling of a Buck Converter using State Space Averaging for Magnet
[39] Load," *International Journal of Recent Research in Electrical and Electronics Engineering,* vol. 3, no. 3, pp. 11-17, 2016.

[40] Guy Séguier ,Francis Labrique ,Philippe Delarue, Électronique de puissance Structures, commandes,applications, Paris: DUNOD, 2015.

S. S. F. K. B. T. A. R. C. Okba Boutebba, "Robust Non-Linear Controller Design for DC-DC Buck
[41] converter via Modified Back-Stepping Methodology," *Elektronika IR Elektrotechnika,* vol. 28, no. 6, 2022.

Sathish Kumar Kollimalla, Student Member, IEEE and Mahesh Kumar Mishra, Senior Member,
[42] IEEE, A Novel Adaptive P&O MPPT Algorithm Considering Sudden Changes in the Irradiance, IEEE Transactions On Energy Conversion, 2014.